Chapter 7
Control of Haptic Systems

Thomas Opitz and Oliver Meckel

Abstract This chapter reviews some aspects of the control of haptic systems, including advanced forms of technical descriptions, system stability criteria and measures, as well as the design of different control laws. A focus is set on the control of bilateral teleoperation systems including the derivation of control designs that guarantee stability as well as haptic transparency and the handling of time delay in the control loop. The chapter also includes an example for the consideration of thermal properties and non-ideal mechanics in the control of a linear stage made from an EC motor and a ball screw as well as a perception-orientated approach to haptic transparency intended to lower the technical requirements on the control and component design.

The control of technical systems aims at safe and reliable system behavior, and controllable system states. By its depiction as a *system*, the analysis is put on an abstracted level, which allows covering many different technical systems described by their fundamental physics. On this abstracted level, a general analysis of closed-loop control issues is possible using several methods and techniques. The resulting procedures are applicable to a large number of system classes. The main purpose of any depiction and analysis of control systems is to achieve high performance, safe system behavior, and reliable processes. Of course, this also holds for haptic systems. Here, stable system behavior and high transparency are the most important control law design goals. The abstract description used for a closed-loop control analysis starts with the mathematical formulation of the physical principles the system fol-

T. Opitz (✉)
Institute of Electromechanical Design, Technische Universität Darmstadt,
Merckstr. 25, 64283 Darmstadt, Germany
e-mail: t.opitz@hapticdevices.eu

O. Meckel
Wittenstein Motion Control GmbH, Igersheim, Germany
e-mail: o.meckel@hapticdevices.eu

C. Hatzfeld and T.A. Kern (eds.), *Engineering Haptic Devices*,
Springer Series on Touch and Haptic Systems, DOI 10.1007/978-1-4471-6518-7_7

lows. As mentioned above, systems with different physical principles are covered up by similar mathematical methods. The depiction by differential equations or systems of differential equations proves widely usable for the formulation of various system behaviors. Herein, analogies allow transforming this system behavior into the different technical contexts of different systems, provided there exists a definite formulation of the system states that are of interest for closed-loop control analysis. The mathematical formulation of the physical principles of the system, also denoted as modeling, is followed by system analysis including dynamic behavior and its characteristics. With this knowledge, a wide variety of design methods for control systems become applicable. Their main requirements are:

System stability The fundamental requirement for stability in any technical system is the main purpose for closed-loop control design. For haptic systems, stability is the most important criteria to guarantee safe use of the device for the user.

Control quality Tracking behavior of the system states to demanded values, every system is faced with external influences also denoted as disturbances that interfere with the demanded system inputs and disrupt the optimal system behavior. To compensate this negative influence, a control system is designed.

Dynamic behavior and performance In addition to the first two issues, the need for a certain system dynamics completes this requirement list. With a view to haptic systems, the focus lies on the transmitted mechanical impedance which determines the achievable grade of transparency.

Besides the quality of the control result tracking the demanded values, the system behavior within the range of changes from these demanded values is focused. Also, the control effort that needs to achieve a certain control result is to be investigated. The major challenge for closed-loop control law design for haptic systems and other engineering disciplines is to deal with different goals that are often in conflict with each other. Typically, a gained solution is never an optimal one, rather a trade-off between system requirements. In the following Sect. 7.1, basic knowledge of linear and nonlinear system description is given. Section 7.2 gives a short overview of system stability analysis. A recommendation for structuring the control law design process for haptic systems is given in Sect. 7.3. Subsequently, Sect. 7.4 focuses on common system descriptions for haptic systems and shows methods for designing control laws. Closing in Sect. 7.5, a conclusion is presented.

7.1 System Description

A variety of description methods can be applied for mathematical formulation of systems with different physical principles. One of the main distinctions is drawn between methods for the description of linear and nonlinear systems, summarized in the following paragraphs. The description based on single-input–single-output (SISO) systems in the LAPLACE domain was discussed in Sect. 4.3.

7.1.1 Linear State Space Description

Besides the formulation of system characteristics through transfer functions, the description of systems using state space representation in the time domain also allows to deal with arbitrary linear systems. For SISO systems, a description using an nth-order ordinary differential equation is transformable into a set with n first-order ordinary differential equations. In addition to the simplified use of numerical algorithms for solving this set of differential equations, the major advantage is applicability to multi-input–multi-output (MIMO) systems. A correct and systematic model of their coupled system inputs, system states, and system outputs is comparably easy to achieve. In contrast to the system description in the LAPLACE domain by transfer functions $G(s)$, the state space representation formulates the system behavior in the time domain. Two sets of equations are necessary for a complete state space system representation. These are denoted as the *system equation*

$$\dot{\mathbf{x}} = \mathbf{A}\mathbf{x} + \mathbf{B}\mathbf{u} \tag{7.1}$$

and the *output equation*

$$\mathbf{y} = \mathbf{C}\mathbf{x} + \mathbf{D}\mathbf{u}. \tag{7.2}$$

The vectors **u** and **y** describe the multidimensional system input, respectively, to system output. Vector **x** denotes the inner system states.

As an example for state space representation, the second-order mechanical oscillating system as shown in Fig. 7.1 is examined. Assuming the existence of time invariant parameters, the description using second-order differential equation is

$$m\ddot{y} + d\dot{y} + ky = u \tag{7.3}$$

The transformation of the second-order differential Eq. (7.3) into a set of two first-order differential equations is done by choosing the integrator outputs as system states:

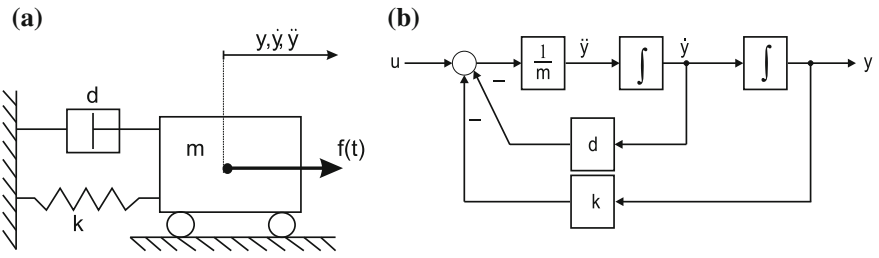

Fig. 7.1 Second-order oscillator **a** scheme, **b** block diagram

$$x_1 = y \Rightarrow \dot{x}_1 = x_2$$
$$x_2 = \dot{y} \Rightarrow \dot{x}_2 = -\frac{k}{m}x_1 - \frac{d}{m}x_2 + \frac{1}{m}u \tag{7.4}$$

Thus, the system equation for state space representation is as follows:

$$\begin{bmatrix} \dot{x}_1 \\ \dot{x}_2 \end{bmatrix} = \begin{bmatrix} 0 & 1 \\ -\frac{k}{m} & -\frac{d}{m} \end{bmatrix} \begin{bmatrix} x_1 \\ x_2 \end{bmatrix} + \begin{bmatrix} 0 \\ \frac{1}{m} \end{bmatrix} u \tag{7.5}$$

The general form of the system equation is

$$\dot{\mathbf{x}} = \mathbf{A}\mathbf{x} + \mathbf{B}\mathbf{u} \tag{7.6}$$

This set of equations contains the *state space vector* **x**. Its components describe all inner variables of the process that are of interest and that have not been examined explicitly using a formulation by transfer function. The system output is described by the output equation. In the given example as shown in Fig. 7.1, the system output y is equal to the inner state x_1

$$y = x_1 \tag{7.7}$$

which leads to the vector representation of

$$y = \begin{bmatrix} 1 & 0 \end{bmatrix} \begin{bmatrix} x_1 \\ x_2 \end{bmatrix} \tag{7.8}$$

The general form of the output equation is

$$\mathbf{y} = \mathbf{C}\mathbf{x} + \mathbf{D}\mathbf{u} \tag{7.9}$$

which leads to the general state space representation applicable for single- or multi-input and output systems. The structure of this representation is depicted in Fig. 7.2. Although not mentioned in this example, matrix **D** denotes a direct feedthrough, which occurs in systems whose output signals y are directly affected by the input signals u without any time delay. Thus, these systems show a non-delayed step response. For further explanation on A, B, C, and D, [32] is recommended. Note that in many teleoperation applications where long distances between master device and slave device exist, significant time delays occur.

7.1.2 Nonlinear System Description

A further challenge within the formulation of system behavior is to imply nonlinear effects, especially if a subsequent system analysis and classification is needed. Although a mathematical description of nonlinear system behavior might be found

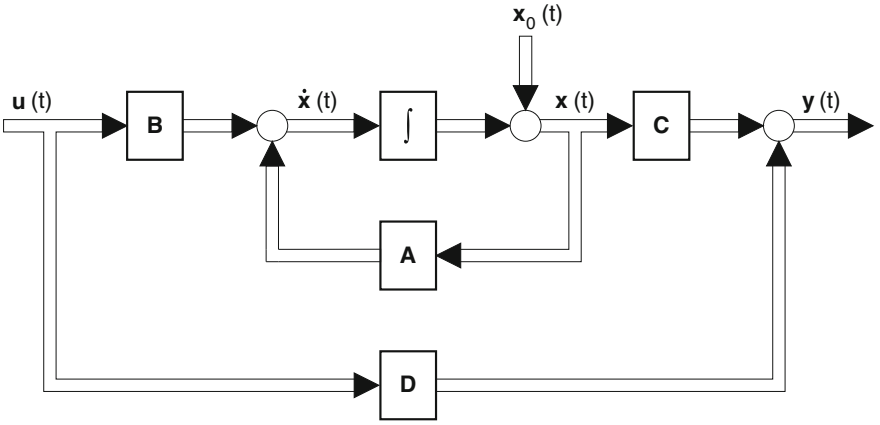

Fig. 7.2 State space description

Fig. 7.3 WIENER-model

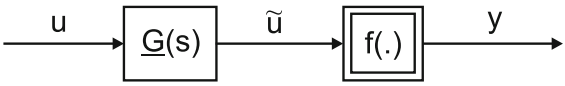

Fig. 7.4 HAMMERSTEIN-model

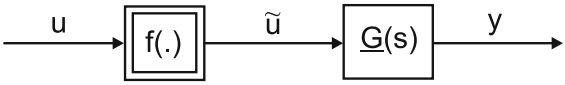

fast, the applicability of certain control design methods is an additional problem. Static nonlinearities can be easily described by serial coupling of a static nonlinear and linear dynamic device to be used as a summarized element for closed-loop analysis. Herein, two different models are differentiated. Figure 7.3 shows the block diagram of a linear element with arbitrary subsystem dynamics followed by a static nonlinearity.

This configuration also known as WIENER-model is described as

$$\tilde{u}(s) = \underline{G}(s) \cdot u(s)$$
$$y(s) = f(\tilde{u}(s)).$$

In comparison, Fig. 7.4 shows the configuration of the HAMMERSTEIN-*model* changing the order of the underlying static nonlinearity and the linear dynamic subsystem.

The corresponding mathematical formulation of this model is described as

$$\tilde{u}(s) = f(u(s))$$
$$y(s) = \underline{G}(s) \cdot \tilde{u}(s).$$

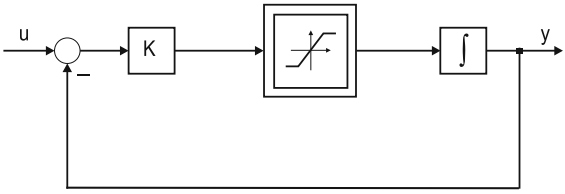

Fig. 7.5 System with internal saturation

More complex structures appear as soon as the dynamic behavior of a system is affected by nonlinearities. Figure 7.5 shows as an example a system with internal saturation. For this configuration, both models cannot be applied as easily as for static nonlinearities, in particular, if a system description is needed usable for certain methods of system analysis and investigation.

Typical examples for systems showing such nonlinear behavior are electrical motors whose torque current characteristic is affected by saturation effects and thus whose torque available for acceleration is limited to a maximum value.

This kind of system behavior is one example of how complicated the process of system modeling may become, as ordinary linear system description methods are not applicable to such a case. Nevertheless, it is necessary to gain a system formulation in which the system behavior and system stability can be investigated successfully. To achieve a system description taking various system nonlinearities into account, it is recommended to set up nonlinear state space descriptions. They offer a wide set of tools applicable to the following investigations. Deriving from Eqs. (7.1) and (7.2), the nonlinear system description for single-, multi-input, and output systems is as follows:

$$\dot{\mathbf{x}} = \mathbf{f}(x, \mathbf{u}, t)$$
$$\mathbf{y} = \mathbf{g}(x, \mathbf{u}, t).$$

This state space description is most flexible to gain a usable mathematical formulation of a systems behavior consisting of static, dynamic, and arbitrarily coupled nonlinearities. In the following, these equations serve as a basis for the examples illustrating concepts of stability and control.

7.2 System Stability

As mentioned above, one of the most important goals of control design is the stabilization of systems or processes during their life cycle, while operative or disabled. Due to the close coupling of haptic systems with a human user via a human–machine interface, safety becomes most relevant. Consequently, the focus of this chapter lies on system stability and its analysis using certain methods applicable to many systems. It must resemble the system behavior correctly and must be aligned with the applied investigation technique. For the investigation of systems, subsystems, close-looped systems, and single- or multi-input output systems, a wide variety of methods exist. The most important ones are introduced in this chapter.

7.2.1 Analysis of Linear System Stability

The stability analysis of linear time invariant systems is easily done by investigation of the system poles or roots derived from the eigenvalue calculation of the system transfer function $G(s)$. The decisive factor is the sign of the real part of these system poles. A negative sign in this real part indicates a stable eigenvalue; a positive sign denotes an unstable eigenvalue. The correspondence to the system stability becomes obvious while looking at the homogeneous part of the solution of the ordinary differential equation describing the system behavior. For example, a system is described as

$$T\dot{y}(t) + y(t) = Ku(t). \tag{7.10}$$

The homogeneous part of the solution $y(t)$ is derived using

$$y_h = e^{\lambda t} \quad \text{with} \quad \lambda = -\frac{1}{T}. \tag{7.11}$$

As it can be seen clearly, the pole $\lambda = -\frac{1}{T}$ has a negative sign only if the time constant T has a positive sign. In this case, the homogeneous part of $y(t)$ disappears for $t \to \infty$, while it rises beyond each limit exponentially if the pole $\lambda = -\frac{1}{T}$ is unstable. This section will not deal with the basic theoretical background of linear system stability as these are basics of control theory. The focus of this section is the application of certain stability analysis methods. Herein, it will be distinguished between methods for direct stability analysis of a system or subsystem and techniques of closed-loop stability analysis. For direct stability analysis of linear system, investigation of the poles placement in the complex plane is fundamental. Besides the explicit calculation of the system poles or eigenvalues, the ROUTH- HURWITZ *criterion* offers to determine the system stability and system pole placement with explicit calculation. In many cases, this simplifies the stability analysis. For the analysis of closed-loop stability, determination of closed-loop pole placement is also a possible approach. Additional methods leave room for further design aspects and extend the basic stability analysis. Well-known examples of such techniques are

- Root locus method,
- NYQUIST's stability criterion.

The applicability of both methods are discussed in the following without looking at the exact derivation.

7.2.1.1 Root Locus Method

The root locus offers the opportunity to investigate pole placement in the complex plane depending on certain invariant system parameters. As example of invariant system parameters, changing time constants or variable system gains might occur. The gain of the open loop is often of interest within the root locus method for

closed-loop stability analysis and control design. In Eq. (7.12), G_R denotes the transfer function of the controller and G_S describes the behavior of the system to be controlled.

$$-G_o = G_R G_S \tag{7.12}$$

Using the root locus method, it is possible to apply predefined sketching rules whenever the dependency of the closed-loop pole placement on the open-loop gain K is of interest. The closed-loop transfer function G_g is depicted by Eq. (7.13)

$$G_g = \frac{G_R G_S}{1 + G_R G_S} \tag{7.13}$$

As an example, an integrator system with a second-order delay (IT_2) described by Eq. (7.14)

$$G_S = \frac{1}{s} \cdot \frac{1}{1+s} \cdot \frac{1}{1+4s} \tag{7.14}$$

is examined. The control transfer function is $G_R = K_R$. Thus, we find as open-loop transfer function

$$-G_o = G_R G_S = \frac{K_R}{s(1+s)(1+4s)}. \tag{7.15}$$

Using the sketching rules that can be found in various examples in the literature [33, 43], the root locus graph as shown in Fig. 7.6 is derived. The graph indicates that small gains K_R lead to a stable closed-loop system since all roots have a negative real part. A rising K_R leads to two of the roots crossing the imaginary axis and the closed-loop system becomes unstable. This simplified example proves that this method can be integrated in a control design process, as it delivers a stability analysis of the closed-loop system by only processing an examination on the open-loop system. This issue is also one of the advantages of the NYQUIST stability criterion. Additionally, the definition of the open-loop system is sufficient to derive a stability analysis of the system in a closed-loop arrangement.

7.2.1.2 NYQUIST's Stability Criterion

This section concentrates on the simplified NYQUIST stability criterion investigating the open-loop frequency response described as

$$-G_o(j\omega) = G_R(j\omega) G_S(j\omega).$$

The NYQUIST stability criterion is based on the characteristic correspondence of amplitude and phase of the frequency response. As example, we use the already introduced IT_2 system controlled by a proportional controller $G_R = K_R$. The BODE plot of the frequency response is shown in Fig. 7.7. The stability condition that has

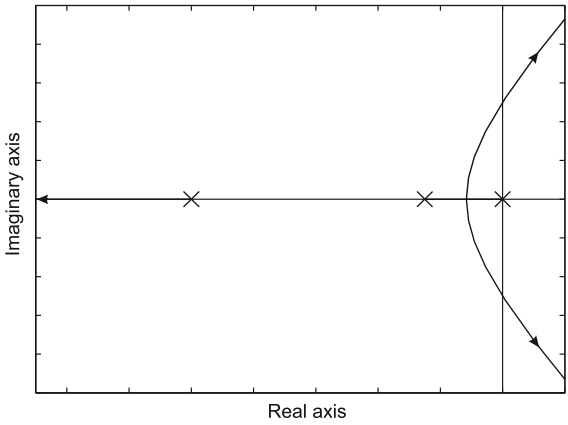

Fig. 7.6 IT_2 root locus

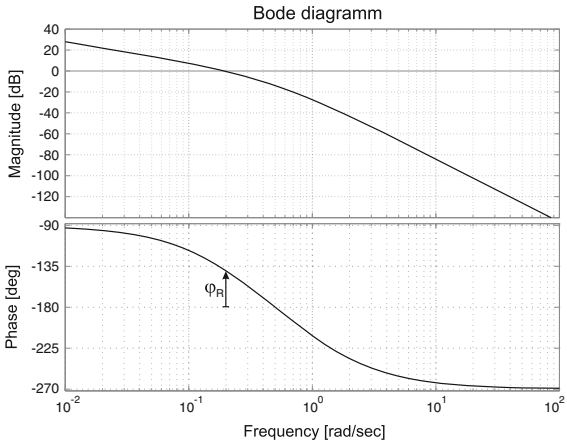

Fig. 7.7 IT_2 frequency response

to be met is given by the phase of the open-loop frequency response, with $\varphi(\omega) > -180°$ in case of the frequency response's amplitude $A(\omega)$ being above 0 dB. As shown in Fig. 7.7, the choice of the controller gain K_R transfers the amplitude graph of the open-loop frequency response vertically without affecting the phase of the open-loop frequency response. For most applications, the specific requirement of a sufficient phase margin φ_R is compulsory. The resulting phase margin is also shown in Fig. 7.7. All such requirements have to be met in the closed-control loop and must be determined to choose the correct control design method. In this example, the examined amplitude and phase of the open-loop frequency response are dependent on the proportional controller gain K_R, which is sufficient to establish system stability including a certain phase margin. More complex control structures such as PI, $PIDT_n$, or lead lag extend the possibilities for control design to meet further requirements.

This section shows the basic principle of the simplified NYQUIST criterion applicable to stable open-loop systems. For investigation of unstable open-loop systems, the

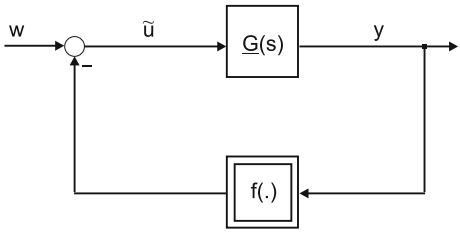

Fig. 7.8 Nonlinear closed-loop system

general form of the NYQUIST criterion must be used, which itself is not introduced in this book. For this basic knowledge, it is recommended to consult [33, 43].

7.2.2 Analysis of Nonlinear System Stability

The application of all previous approaches for the analysis of system stability is limited to linear time invariant systems. Nearly all real systems show nonlinear effects or consist of nonlinear subsystems. One approach to deal with these nonlinear systems is linearization in a fixed working point. All further investigations are focused on this point, and the application of the previously presented methods becomes possible. If these methods are not sufficient, extended techniques for stability analysis of nonlinear systems must be applied. The following are examples of representing completely different approaches:

- Principle of harmonic balance;
- Phase plane analysis;
- POPOV criterion and circle criterion;
- LYAPUNOV's direct method;
- System passivity analysis.

Without dealing with the mathematical background or the exact proof, the principles and application of the chosen techniques are demonstrated. At this point, a complete explanation of this topic is too extensive due to the wide variety of underlying methods. For further detailed explanation, [13–15, 29, 39, 42] are recommended.

7.2.2.1 POPOV Criterion

As preliminary example, the analysis of closed-loop systems can be done applying the POPOV criterion, respectively, the circle criterion. Figure 7.8 shows the block diagram of the corresponding closed-loop structure of the system to be analyzed:

The block diagram consists of a linear transfer function $\underline{G}(s)$ with arbitrary dynamics and static nonlinearity $f(.)$. The state space formulation of $\underline{G}(s)$ is as follows:

$$\dot{\mathbf{x}} = \mathbf{A}\mathbf{x} + \mathbf{B}\tilde{u}$$
$$\mathbf{y} = \mathbf{C}\mathbf{x}$$

Thus, we find for the closed-loop system description:

$$\dot{\mathbf{x}} = \mathbf{A}\mathbf{x} - \mathbf{B}f(y)$$
$$y = \mathbf{C}\mathbf{x}.$$

In case $f(y) = k \cdot y$, this nonlinear system is reduced to a linear system whose stability can be examined with the evaluation of the system's eigenvalues. For an arbitrary nonlinear function $f(y)$, the complexity of the problem is extended. So, the first constraint on $f(y)$ is that it exists only in a determined sector limited by a straight line through the origin with gradient k. Figure 7.9 shows an equivalent example for the nonlinear function $f(y)$. This constraint is depicted by the following equation:

$$0 \leq f(y) \leq ky.$$

The POPOV criterion provides an intuitive handling for the stability analysis of the presented example. The system is asymptotically idle state ($\dot{\mathbf{x}} = \mathbf{x} = \mathbf{0}$) stable if:

- the linear subsystem $\underline{G}(s)$ is asymptotically stable and fully controllable,
- the nonlinear function meets the presented sector condition as shown in Fig. 7.9,
- for an arbitrarily small number $\rho \geq 0$, there exists a positive number α, so that the following inequality is satisfied:

$$\forall\omega \geq 0 \quad \mathrm{Re}[(1 + j\alpha\omega)\underline{G}(j\omega)] + \frac{1}{k} \geq \rho \tag{7.16}$$

Equation (7.16) formulates the condition also known as POPOV *inequality*. With

$$\underline{G}(j\omega) = \mathrm{Re}(\underline{G}(j\omega)) + j\mathrm{Im}(\underline{G}(j\omega)) \tag{7.17}$$

Equation (7.16) leads to

$$\mathrm{Re}(\underline{G}(j\omega)) - \alpha\omega\mathrm{Im}(\underline{G}(j\omega)) + \frac{1}{k} \geq \rho \tag{7.18}$$

With an additional definition of a related transfer function

$$G^* = \mathrm{Re}(\underline{G}(j\omega)) + j\omega\mathrm{Im}(\underline{G}(j\omega)), \tag{7.19}$$

Equation (7.18) states that the plot in the complex plane of $\underline{G}^*$, the so-called POPOV *plot*, has to be located in a sector with an upper limit described as $y = \frac{1}{\alpha}(x + \frac{1}{k})$. Figure 7.10 shows an example for the POPOV plot of a system in the complex plane constrained by the sector condition. The close relation to the NYQUIST criterion for

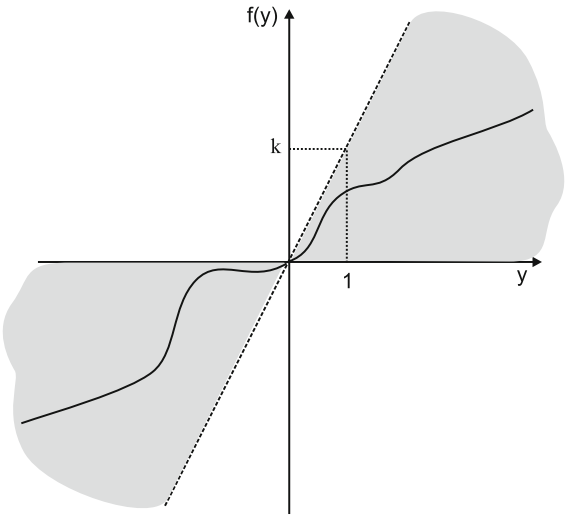

Fig. 7.9 Sector condition

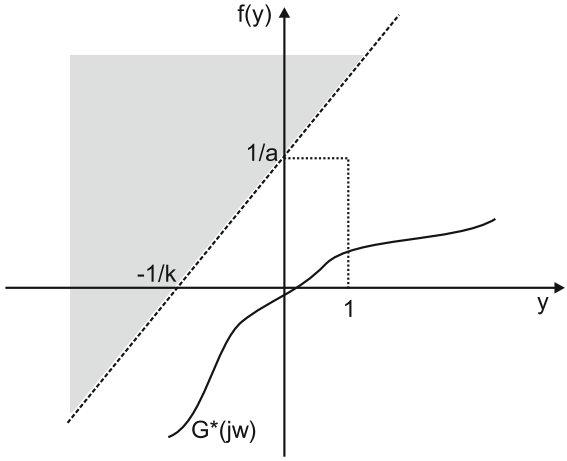

Fig. 7.10 POPOV plot

the stability analysis of linear systems becomes obvious here. While the NYQUIST criterion examines the plot of $\underline{G}(j\omega)$ referred to the critical point $(-1|0)$, the location of the POPOV plot is checked for a sector condition defined by a straight line limit.

The application of the POPOV criterion has the excellent advantage that it is possible to gain a result out of the stability analysis without an exact formulation of the nonlinearity within the system. All constraints for the nonlinear subsystem are restrained to the sector condition and the condition to have memoryless transfer behavior. The most complicated aspect within this kind of analysis is how to formulate the considered system structure in a way that the POPOV criterion can be applied. For completeness, the circle criterion is mentioned whose sector condition is not

represented by a straight line, rather

$$k_1 \leq \frac{f(y)}{y} \leq k_2.$$

defines the new sector condition. For additional explanation on these constraints and the application of the circle criterion, it is recommended to consider [29, 39, 42].

7.2.2.2 LYAPUNOV's Direct Method

As a second example for stability analysis of nonlinear systems, the direct method of LYAPUNOV is introduced. The basic principle is that if both linear and nonlinear stable systems tend to a stable steady state, the complete system energy has to be dissipated continuously. Thus, it is possible to gain a result from stability analysis while verifying the characteristics of the function representing the state of energy in the system. LYAPUNOV's direct method generalizes this approach to evaluate the system energy by generation of an artificial scalar function, which can describe not only the energy stored within the considered dynamic system, but is also used as an energy-like function of a dissipative system. Such functions are called LYAPUNOV functions $V(x)$. For the examination of the system stability, the aforementioned state space description of a nonlinear system is used:

$$\begin{aligned} \dot{x} &= f(x, u, t) \\ y &= g(x, u, t). \end{aligned}$$

By the definition of LYAPUNOV's theorem, the equilibrium at the phase plane origin $\dot{\mathbf{x}} = \mathbf{x} = \mathbf{0}$ is globally, asymptotically stable if

1. a positive definite scalar function $V(\mathbf{x})$ with $\mathbf{x}$ as the system state vector exists, meaning that $V(\mathbf{0}) = 0$ and $V(\mathbf{x}) > 0 \,\forall\, \mathbf{x} \neq \mathbf{0}$,
2. $\dot{V}$ is negative definite, meaning $\dot{V}(\mathbf{x}) \leq 0$,
3. $V(\mathbf{x})$ is not limited, meaning $V(\mathbf{x}) \to \infty$ as $\| x \| \to \infty$.

If these conditions are met in a bounded area at the origin only, the system is locally asymptotically stable.

As a clarifying example, the following nonlinear first-order system

$$\dot{x} + fx = 0 \tag{7.20}$$

is evaluated. Herein, $f(x)$ denotes any continuous function of the same sign as its scalar argument x so that $x \cdot fx > 0$ and $f(0) = 0$. Applying this constraint, a LYAPUNOV function candidate can be found described as

$$V = x^2. \tag{7.21}$$

The time derivative of $V(x)$ provides

$$\dot{V} = 2x\dot{x} = -2xf(x). \tag{7.22}$$

Due to the assumed characteristics of $f(x)$, all conditions of LYAPUNOV's direct method are satisfied; thus, the system has globally, asymptotically stable equilibrium at the origin. Although the exact function $f(x)$ is not known, the fact that it exists in the first and third quadrants only is sufficient for $\dot{V}(x)$ to be negative definite. As second example, a MIMO system is examined depicted by its state space formulation

$$\begin{aligned}\dot{x}_1 &= x_2 - x_1(x_1^2 + x_2^2)\\ \dot{x}_2 &= -x_1 - x_2(x_1^2 + x_2^2).\end{aligned}$$

In this example, the system has an equilibrium at the origin too. Consequently, the following LYAPUNOV function candidate can be found:

$$V(x_1, x_2) = x_1^2 + x_2^2. \tag{7.23}$$

Thus, the corresponding time derivative is

$$\dot{V}(x_1, x_2) = 2x_1\dot{x_1} + 2x_2\dot{x_2} = -2(x_1^2 + x_2^2)^2. \tag{7.24}$$

Hence, $V(x_1, x_2)$ is positive definite and $\dot{V}(x_1, x_2)$ is negative definite. Thus, the equilibrium at the origin is globally, asymptotically stable for the system.

A difficult aspect when using the LYAPUNOV direct method is given by how to find LYAPUNOV function candidates. No straight algorithm with a determined solution exists, which is a disadvantage of this method. SLOTINE AND LE [39] propose several structured approaches to gain LYAPUNOV function candidates, namely

- KRASOVSKII's method and
- the variable gradient method.

Besides these, SLOTINE provides additional possibilities to involve the system's physical principles in the procedure for determining of LYAPUNOV function candidates while analyzing more complex nonlinear dynamic systems.

7.2.2.3 Passivity in Dynamic Systems

As another method for the stability analysis of dynamic systems, the passivity formalism is introduced within this section. Functions can be extended to system combinations using LYAPUNOV's direct method and evaluating the dissipation of energy in dynamic systems. The passivity formalism is also based on nonlinear positive definite storage functions $V(\mathbf{x})$ with $V(\mathbf{0} = \mathbf{0})$ representing the overall system energy. The time derivative of this energy determines the system's passivity. As example, the general formulation of a system

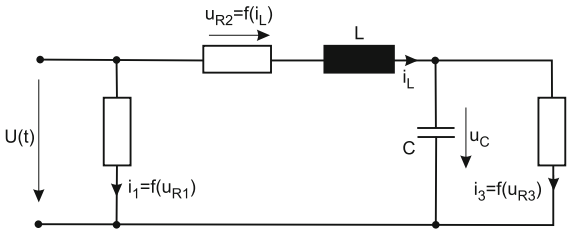

Fig. 7.11 Passivity analysis of an RLC-network

$$\dot{x} = f(x, u, t)$$
$$y = g(x, u, t).$$

is considered. This system is passive concerning the external supply rate $S = \mathbf{y}^T\mathbf{u}$ if the inequality condition

$$\dot{V}(\mathbf{x}) \leq \mathbf{y}^T\mathbf{u} \tag{7.25}$$

is satisfied. KHALIL distinguishes several cases of system passivity depending on certain system characteristics (*Lossless, Input Strictly Passive, Output Strictly Passive, State Strictly Passive, Strictly Passive*) [29]. If a system is passive concerning the *external supply rate S*, it is stable in the sense of LYAPUNOV.

The combination of passive systems using parallel or feedback structures inherits the passivity from its passive subsystems. With the close relation of system passivity to stability in the sense of LYAPUNOV, the examination of system stability is possible by verifying the subsystem's passivity. Based on this evaluation, it can be concluded that the overall system is passive—always with the assumption that a correct system structure was built.

As an illustrating example, the RLC circuit taken from [29] is analyzed in the following. The circuit structure is shown in Fig. 7.11.

The system's state vector is defined as

$$i_L = x_1$$
$$u_C = x_2.$$

The input u represents the supply voltage U, as output y the current i is observed. The resistors are described by the corresponding voltage current characteristics:

$$i_1 = f_1(u_{R1})$$
$$i_3 = f_3(u_{R3})$$

For the resistor that is coupled in series with the inductor, the following behavior is assumed:

$$U_{R2} = f_2(i_L) = f_2(x_1). \tag{7.26}$$

Thus, the nonlinear system is described by the differential equation:

$$\begin{aligned} L\dot{x_1} &= u - f_2(x_1) - x_2 \\ C\dot{x_2} &= x_1 - f_3(x_2) \\ y &= x_1 + f_1(u) \end{aligned}$$

The presented RLC circuit is passive as long as the condition

$$V(\mathbf{x}(t)) - V(\mathbf{x}(0)) \leq \int_0^t u(\tau)y(\tau)\mathrm{d}\tau \tag{7.27}$$

is satisfied. In this example, the energy stored in the system is described by the storage function

$$V(\mathbf{x}(t)) = \frac{1}{2}Lx_1^2 + \frac{1}{2}Cx_2^2. \tag{7.28}$$

Equation 7.27 leads to the condition for passivity:

$$\dot{V}(\mathbf{x}(t), u(t)) \leq u(t)y(t) \tag{7.29}$$

which means that the energy supplied to the system must be equal to or higher than the time derivative of the energy function. Using $V(\mathbf{x})$ in the condition for passivity provides

$$\begin{aligned} \dot{V}(\mathbf{x}, u(t)) &= Lx_1\dot{x_1} + Cx_2\dot{x}_2 \\ &= x_1\left(u - f_2(x_1) - x_2\right) + x_2\left(x_1 - f_3(x_2)\right) \\ &= x_1\left(u - f_2(x_1)\right) + x_2 f_3(x_2) \\ &= \left(x_1 + f_1(u)\right)u - uf_1(u) - x_1 f_2(x_1) - x_2 f_3(x_2) \\ &= uy - uf_1(u) - x_1 f_2(x_1) - x_2 f_3(x_2) \end{aligned}$$

and finally

$$u(t)y(t) = \dot{V}(\mathbf{x}, u(t)) + uf_1(u) + x_1 f_2(x_1) + x_2 f_3(x_2). \tag{7.30}$$

In case f_1, f_2, and f_3 are passive subsystems, i.e., all functions describing the corresponding characteristics of the resistors exist only in the first and third quadrants, then $\dot{V}(\mathbf{x}, u(t)) \leq u(t)y(t)$ is true; hence, the RLC circuit is passive. Any coupling of this passive system to other passive systems in parallel or feedback structures again results in a passive system. For any passivity analysis and stability evaluation, this method implements a structured procedure and shows high flexibility.

In conclusion, it is necessary to mention that all methods for stability analysis introduced in this section show certain advantages and disadvantages concerning their applicability, information value, and complexity, regardless of whether linear

or nonlinear systems are considered. When a stability analysis is expected to be done, the applicability of a specific method should be checked individually. This section gives a brief overview of the introduced methods and techniques and does not claim to be a detailed description due to the limited scope of this section. For further study, the reader is invited to consult the proposed literature.

7.3 Control Law Design for Haptic Systems

As introduced at the beginning of this chapter, control design is a fundamental and necessary aspect within the development of haptic systems. In addition to the techniques for system description and stability analysis, the need for control design and the applicable design rules becomes obvious. For control design of a haptic system, it is especially necessary to deal with several aspects and conditions to be satisfied during the design process. The following sections present several control structures and design schemes to set up a basic knowledge of the toolbox for analytic control design of haptic systems. This also involves some of the already introduced methods for system formulation and stability analysis, as they form the basis for most control design methods.

7.3.1 Structuring of Control Design

As introduced in Chap. 6, various structures of haptic systems exist. Demands on the control of these structures are derived in the following.

Open-loop impedance controlled The user experiences an impression of force that is directly commanded via an open loop based only on a demand value. In Chap. 6, the basic scheme of this structure is shown in Fig. 6.1.

Closed-loop impedance controlled As it can be seen in Fig. 6.3, the user also experiences an impression of force that is fed back to a controller. Here, a specific control design is needed.

Open-loop admittance controlled In this scheme, the user experiences an impression of a defined position. In the open-loop arrangement, this position again is directly commanded based only on a demand value. Figure 6.5 shows the corresponding structure of this haptic scheme.

Closed-loop admittance controlled This last version as depicted in Fig. 6.7 shows its significant difference in the feedback of the force the user applies to the interface. This force is fed back to a demand value. This results in a closed-loop arrangement that incorporates the user and his or her transfer characteristics. Different from the closed-loop impedance controlled scheme, this structure uses a force as demanded value $\underline{S}_F$ compared with the detected $\underline{S}_S$, but the system output is still a position $\underline{x}_{\text{out}}$. This results in the fact that the incorporation of the user

into the closed-loop behavior is more complex than in a closed-loop impedance controlled scheme.

All of these structures can be basically implemented in a haptic interaction as shown in Fig. 2.33. From this, all necessary control loops of the overall telemanipulation system become evident:

- On the haptic interface site, a control loop is closed incorporating the user that is valid as long as the user's reaction is fed back to the central interface module for any further data processing or control.
- On the process/environment site also, a closed loop exists if measurable process signals (reactions, disturbances) are fed back to the central interface module for data processing or control.
- Underneath these top-level control loops, various subsystem control loops exist that have a major impact on the overall system too. As an example, each electrical actuator will most likely be embedded in a cascaded control structure with current, speed, and position control.

It becomes obvious that the design of a control system for a telemanipulation system with a haptic interface is complex and versatile. Consequently, a generally valid procedure for control design cannot be given. The control structures must be designed step-by-step involving the following controllers:

1. Design of all controllers for the subsystem actuators;
2. Design of a top-level controller for the haptic interface;
3. Design of a top-level controller for the manipulator/VR environment;
4. Design of the system controller that connects interface and manipulator or VR environment.

This strict separation proposed above might not be the only way to structure the overall system. Depending on the application and functionality, the purposes of the different controller and control levels might be in conflict with each other or might simply overlap. Therefore, it is recommended to set up the underlying system structure and define all applied control schemes corresponding to their required functionality.

While looking at the control of haptic systems, a similar structure can be established. For both the control of the process manipulation and the haptic display or interface, the central interface module will have to generate demand values for force or position that are going to be followed by the controllers underneath. These demand values derive from a calculation predefined by designed control laws. To gain such control laws, a variety of methods and techniques for structural design and optimization can be applied depending on certain requirements. The following sections give an overview of typical requirements to closed-control loop behavior followed by examples for control design.

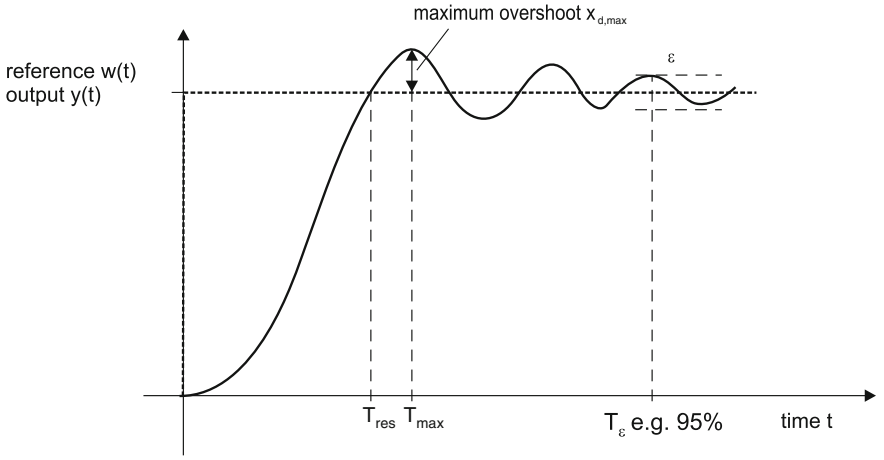

Fig. 7.12 Closed-loop step response requirements

Table 7.1 Parameter for control quality requirements

Parameter	Description
$x_{d,\max}$	Maximum overshoot
$T_{\max}$	Point of time for $x_{d,\max}$
T_ε	Time frame in which the residuum to the demanded value remains within a predefined scope ε
T_{res}	Point of time when the demanded value is reached for the first time

7.3.2 Requirement Definition

Besides the fundamental need for system stability with sufficient stability margins, additional requirements can be set up to achieve a certain system behavior in a closed-loop scheme such as dynamic or precision. A quantitative representation of these requirements can be made by the achievement of certain characteristics of the closed-loop step response.

Figure 7.12 shows the general form of a typical closed-loop step response and its main characteristics. As it can be seen, the demanded value is reached and the basic control requirement is satisfied.

Additional characteristics are discussed and listed in Table 7.1. For all mentioned characteristics, a quantitative definition of certain requirements is possible. For example, the number and amplitude of overshoots shall not extend a defined limit or have a certain frequency spectrum that is of special interest for the control design in haptic systems. As analyzed in Chap. 3, the user's impedance shows a significant frequency range that must not be excited within the control loop of the haptic device. Nevertheless, a certain cut-off frequency has to be reached to establish a good performance of

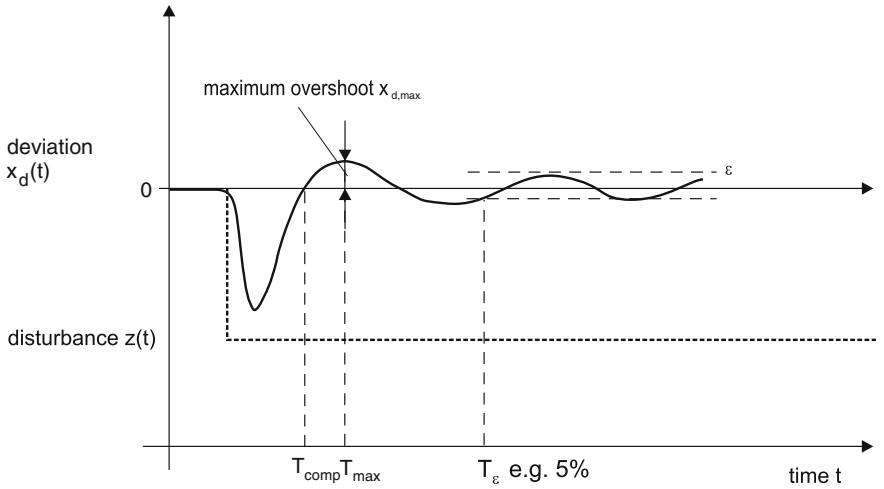

Fig. 7.13 Closed-loop disturbance response requirements

the dynamic behavior. All these issues are valid for requirements to the control design of the process manipulation. In addition to the requirements from the step response due to changes in the setpoint value, it is necessary to formulate requirements concerning the closed-loop system behavior considering disturbances originating from the process. When interpreting the user's reaction as disturbance within the overall system description, a requirement set up for the disturbance reaction of the control loop has to be established. As can be seen in Fig. 7.13, similar characteristics exist to determine the disturbance reaction quantitatively and qualitatively. In most cases, both the step response behavior and the disturbance reaction cannot satisfy all requirements, as they often come into conflict with each other, caused by the limited flexibility of the applied optimization method. Thus, it is recommended to estimate the relevance of step response and disturbance reaction in order to choose an optimization approach that is most beneficial. Although determined quantitatively, it is not possible to use all requirements in a predefined optimization method. In most cases, an adjustment of requirements is necessary to be made, to apply specific control design and optimization methods. As an example, the time T_{res} as depicted above cannot be used directly and must be transferred into a requirement for the closed-loop dynamic characterized by a definite pole placement.

Furthermore, simulation techniques and tests offer iteration within the design procedure to gain an optimal control law. However, this very sufficient way of analyzing system behavior and test designed control laws suggests to forget about the analytic system and control design strategy and switch to a trial an error algorithm.

7.3.3 General Control Law Design

This section presents some possible types of controllers and control structures that might be used in the already discussed control schemes. For optimization of the control parameters, several methods exist, which are introduced here. Depending on the underlying system description, several approaches to set up controllers and control structures are possible. This section presents the classic PID-control, additional control structures, e.g., compensation, state feedback controllers, and observer-based state space control.

7.3.3.1 Classic PID-Control

Maybe, one of the most frequently used controllers is the parallel combination of a proportional (P), an integrating (I) and a derivative (D) controller. This combination is used in several variants including a P-controller, a PI combination, a PD combination, or the complete PID structure. Using the PID structure, all advantages of the individual components are combined. The corresponding controller transfer function is described as

$$\underline{G}_R = K_R \left(1 + \frac{1}{T_N s} + T_V s\right). \tag{7.31}$$

Figure 7.14 shows the equivalent block diagram of a PID controller structure. Adjustable parameters in this controller are the proportional gain K_R, the integrator time constant T_N, and the derivative time T_V.

With optimized parameter adjustment, a wide variety of control tasks can be handled. This configuration offers on the one hand, the high dynamic of the proportional controller and on the other, the integrating component guarantees a high precision step response with a residuum $x_d = 0$ for $t \to \infty$. The derivative finally provides an additional degree of freedom that can be used for a certain pole placement of the closed-loop system.

As major design techniques, the following examples are introduced:

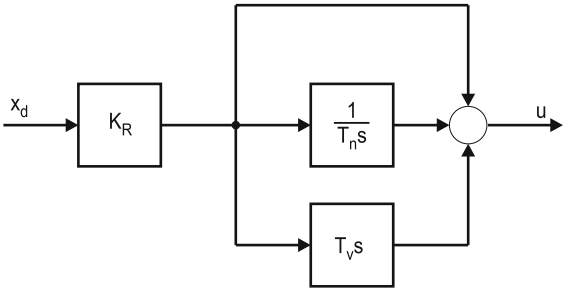

Fig. 7.14 PID block diagram

Root Locus Method This method has its strength by the determined pole placement for the closed-loop system, directly taking into account the dependence on the proportional gain K_R. By a reasonable choice of T_N and T_D, the additional system zeros are influenced that affects directly the resulting shape of the root locus and thus the stability behavior. Besides this, the overall system dynamic can be designed.

Integral Criterion The second method for optimization of the closed-loop system step response or disturbance reaction is the minimization of an integral criterion. The basic procedure for this method is as follows: The tracking error x_d due to changes in the demanded set point or a process disturbance is integrated (and eventually weighted over time). This time integral is minimized by adjusting the controller parameters. In case of convergence of this minimization, the result is a set of optimized controller parameters.

For any additional theoretical background concerning controller optimization, the reader is invited to consult the literature on control theory and control design [32, 33].

7.3.3.2 Additional Control Structures

In addition to the described PID controller, additional control structures extend the influence on the control result without having an impact on the system stability. The following paragraphs present the disturbance compensation and a direct feedforward of auxiliary process variables.

Disturbance Compensation

The basic principle of disturbance compensation assumes that if a disturbance on the process is measurable and its influence is known, this knowledge can be used to establish compensation by corresponding evaluation and processing. Figure 7.15 shows a simplified scheme of this additional control structure.

In this scheme, a disturbance signal is assumed to affect the closed loop via a disturbance z transfer function $\underline{G}_D$. By measuring the disturbance signal and processing, the compensator transfer function $\underline{G}_C$ results in a compensation of the disturbance interference. Assuming an optimal design of the compensator transfer function, this interference caused by the disturbance is completely erased. The optimal design of a corresponding compensator transfer function is depicted as

$$\underline{G}_C = -\frac{\underline{G}_D}{\underline{G}_S}. \tag{7.32}$$

This method assumes that a mathematical and practicable inversion of $\underline{G}_D$ exists. For those cases where this assumption is not valid, the optimal compensator $\underline{G}_K$ must be approximated. Furthermore, Fig. 7.15 states clearly that this additional control

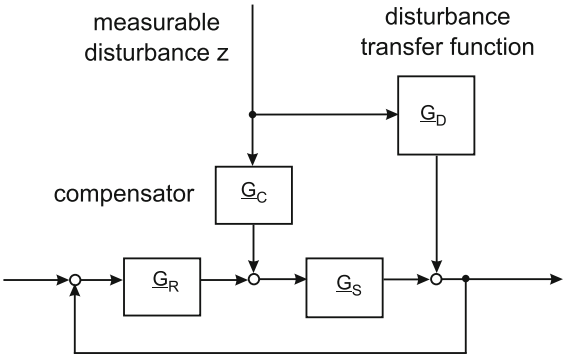

Fig. 7.15 Simplified disturbance compensation

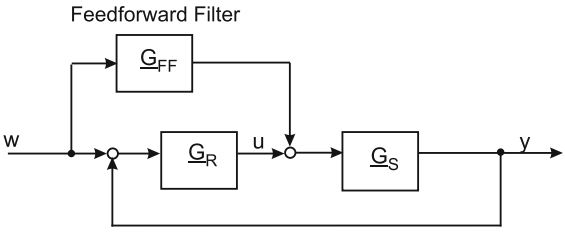

Fig. 7.16 Feedforward of auxiliary input variables

structure does not have any influence on the closed-loop system stability and can be designed independently. Besides, the practicability of the additional effort should be taken into account. This effort will definitively increase just by the sensors to measure the disturbance signals and by the additional costs for realization of the compensator.

Auxiliary Input Feedforward

A structure similar to the disturbance compensation is the *feedforward* of auxiliary input variables. This principle is based on the knowledge of additional process variables that are used to influence the closed-loop system behavior without affecting system stability. Figure 7.16 shows an example of the feedforward of the demanded setpoint w to the controller signal u using a feedforward filter function $\underline{G}_{\mathrm{FF}}$.

7.3.3.3 State Space Control

Corresponding to the techniques for the description of MIMO systems discussed earlier in this chapter, state space control provides additional features to cover the special characteristics within these systems. As described before, MIMO systems are preferably depicted as state space models. Using this mathematical formulation enables the developer to implement a control structure that controls the internal

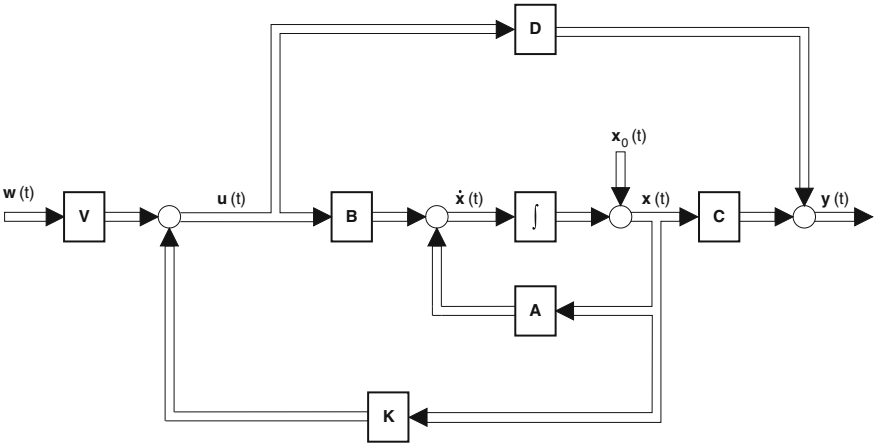

Fig. 7.17 State feedback control

system states to demanded values. The advantage is that the design methods for state space control use an overall approach for control design and optimization instead of a control design step-by-step for each system state. With this approach, it becomes possible to deal with profoundly coupled MIMO systems with high complexity, and design a state space controller simultaneously. This section presents the fundamental state space control structures, which covers the *state feedback control* as well as the *observer-based state space control*. For further detailed procedures as well as design and optimization methods, the reader is referred to [32, 42].

State Feedback Control

As shown in Fig. 7.17, this basic structure for state space control uses a feedback of the system states **x**. Similar to the depiction in Fig. 7.2, the considered system is presented in state space description using matrices **A**, **B**, **C**, and **D**. The system states **x** are fed back gained by the matrix **K** to the vector of the demanded values that were filtered by matrix **V**. The results represent the system input vector u. Both matrices **V** and **K** do not have to be square matrices as a state space description is allowed to implement various dimensions for the state vector, the vector for the demanded values, and the system input vector.

Observer-Based State Space Control

The state space control structure discussed above requires complete knowledge of all system states, which is nothing else but that they have to be measured and processed to be used in the control algorithm. From a practical point of view, this not possible

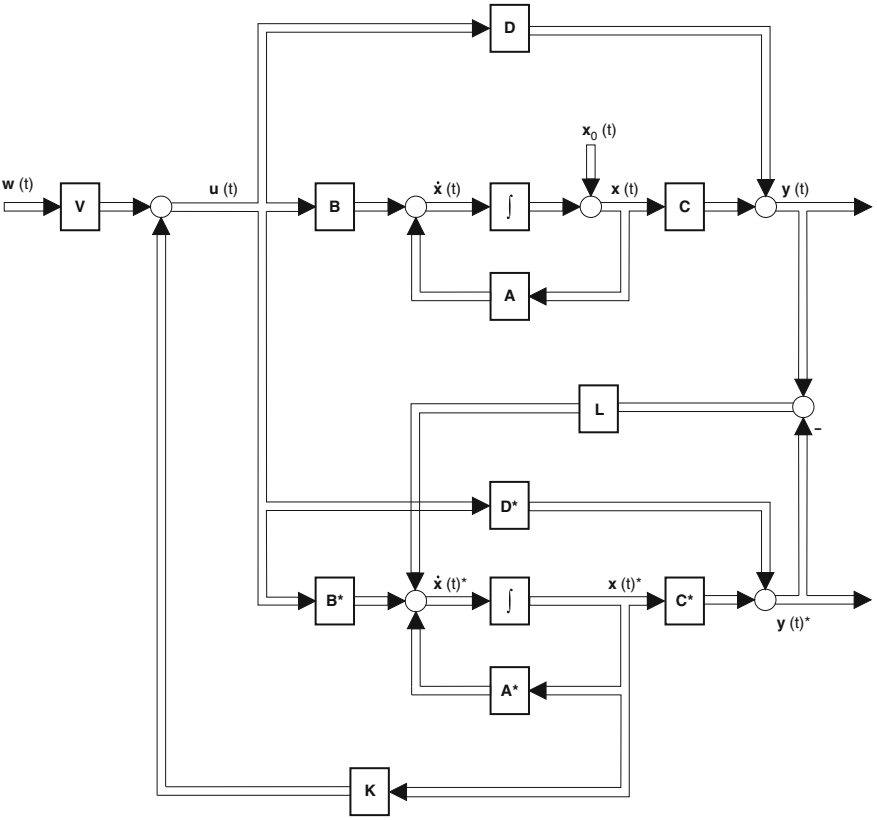

Fig. 7.18 Observer-based state space control

always due to technical limits as well as costs and effort. As a result, the developer is faced with the challenge to establish a state space control without complete knowledge of the system states. As a solution, these system states that cannot be measured due to technical difficulties or significant cost factors estimated using a state space observer structure as shown in Fig. 7.18.

In this structure, a system model is calculated parallel to the real system. As exact as possible, this system model is described by the corresponding parameter matrices $\mathbf{A}^*$, $\mathbf{B}^*$, $\mathbf{C}^*$, and $\mathbf{D}^*$. The model input is also represented by the input vector $\mathbf{u}$. Thus, the model provides an estimation of the real system states $\mathbf{x}^*$ and an estimated system output vector $\mathbf{y}^*$. By comparison of this estimated output vector $\mathbf{y}^*$ with the real output $\mathbf{y}$, which is assumed to be measurable, the estimation error is fed back gained by the matrix $\mathbf{L}$. This results in a correction of the system state estimation $\mathbf{x}^*$. Any estimation error in the system states or the output vector due to varying initial states is corrected and the estimated states $\mathbf{x}^*$ are used to be gained by the equivalent matrix $\mathbf{K}$ and fed back for control.

This structure of an observer-based state space control uses the LUENBERGER observer. In this configuration, all real system states are assumed not to be measurable; thus, the state space control refers to estimated values completely. Practically, the feedback of measurable system states is combined with the observer-based estimation of additional system states. In [32, 42], examples for observer-based state space control structures as well as methods for observer design are discussed in detail.

7.3.4 Example: Cascade Control of a Linear Drive

As an example for the design of a controller, the cascade control of a linear drive buildup of an EC motor and a ball screw is considered in this section based on [27]. The consideration includes nonlinear effects due to friction, temperature change, and a nonlinear degree of efficiency of the ball screw.

A schematic representation of the EC motor is given in Fig. 7.19. in which only one phase is illustrated for simplification. The motor is supplied with voltage u_{DC}. The resistance R and the inductance L represent the stator winding of the motor. The angular speed of the rotor $\underline{\omega}_{\mathrm{M}}$ generates a back electromotive force (back-EMF) u_{EMF}. The mechanical properties of the motor are described by the motor torque $\underline{M}_{\mathrm{e}}$, the load torque $\underline{M}_{\mathrm{L}}$, and the moment of inertia of the rotor J. Mesh analysis yields to the equation for the electrical part of the motor

$$u_{\mathrm{DC}} = Ri + L\frac{\mathrm{d}i}{\mathrm{d}t} + u_{\mathrm{EMF}} \tag{7.33}$$

which can be written in the frequency domain as

$$\underline{U}_{\mathrm{DC}} - \underline{U}_{\mathrm{EMF}} = \underline{I}\,(R + sL) \tag{7.34}$$

The back electromotive force U_{EMF} depends on the angular speed of the rotor ω_M, the back-EMF constant k_e, and the parameter $F(\phi_e)$, which describes the dependence of the back-EMF of the electrical angle ϕ_e.

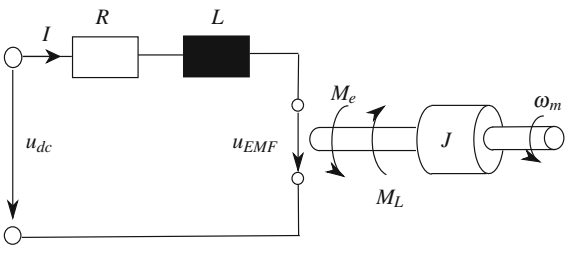

Fig. 7.19 Equivalent circuit of the considered EC motor with attached ball screw to transform rotary into translational movement [27]

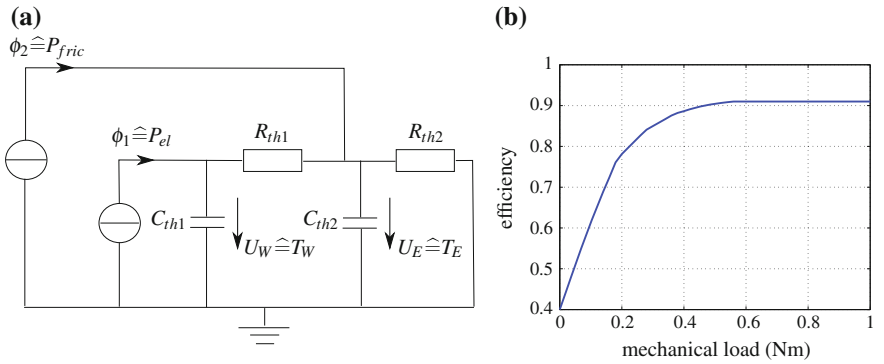

Fig. 7.20 **a** Equivalent thermal circuit of the EC motor, **b** efficiency of the ball screw depending on the mechanical load [27]

$$u_{\mathrm{EMF}} = k_e \omega_{\mathrm{M}} F(\phi_e) \tag{7.35}$$

The motor torque M_{e} generated by the motor current i correlates with the mechanical load M_{L} and the angular acceleration ω_{M} of the rotor with the moment of inertia J. It follows that:

$$M_{\mathrm{e}} = \frac{i \cdot u_{\mathrm{EMF}}}{\omega_{\mathrm{M}}} = i k_{\mathrm{e}} F(\Phi_e) = J \frac{\mathrm{d}\omega_M}{\mathrm{d}t} + M_{\mathrm{L}} \tag{7.36}$$

In the frequency domain, the mechanical properties of the motor are described as

$$M_{\mathrm{e}} - M_{\mathrm{L}} = s J \omega_{\mathrm{M}}. \tag{7.37}$$

The model takes three different types of nonlinearities into account: friction, temperature change, and a nonlinear efficiency of the ball screw. The friction is modeled as the sum of a static friction K_{F} and a dynamic friction $k_{\mathrm{F}} \cdot \omega_{\mathrm{M}}$. So, the equilibrium of moments of the rotor can now be written as

$$M_{\mathrm{e}} - M_{\mathrm{L}} - K_{\mathrm{F}} = (k_{\mathrm{F}} + s J)\omega_{\mathrm{M}}. \tag{7.38}$$

The influence of changes in temperature on motor parameters is modeled by a thermal equivalent circuit shown in Fig. 7.20a. The temperature change in the stator winding T_{W} can be determined by

$$\Delta T_{\mathrm{W}} = \frac{R_{\mathrm{th1}} T_{\mathrm{th2}} s + R_{\mathrm{th1}} R_{\mathrm{th2}}}{T_{\mathrm{th1}} T_{\mathrm{th2}} s^2 + (T_{\mathrm{th1}} + T_{\mathrm{th2}}) s} P_{\mathrm{el}} + \frac{R_{\mathrm{th2}}}{T_{\mathrm{th1}} T_{\mathrm{th2}} s^2 + (T_{\mathrm{th1}} + T_{\mathrm{th2}} + R_{\mathrm{th2}} C_{\mathrm{th1}}) s + 1} P_{\mathrm{fric}}. \tag{7.39}$$

with

$$T_{\mathrm{th1}} = R_{\mathrm{th1}} C_{\mathrm{th1}} \quad \text{and} \quad T_{\mathrm{th2}} = R_{\mathrm{th2}} C_{\mathrm{th2}} \tag{7.40}$$

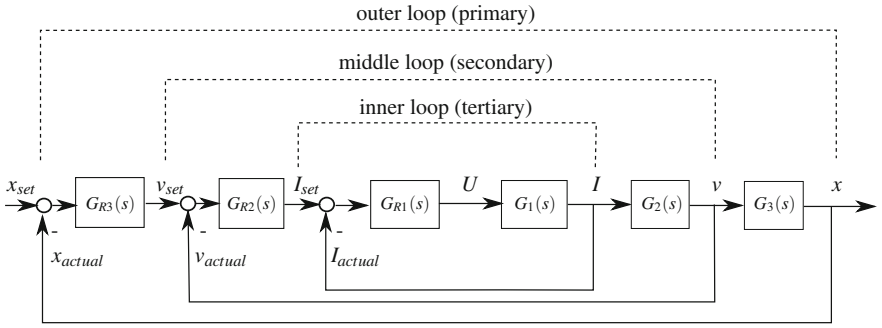

Fig. 7.21 Structure of cascade controller of EC motor [27]

The resulting resistance of the stator winding R_* and the back-EMF constant k_{e*} can be derived with knowledge of the temperature coefficients α_R, α_k from

$$R_* = R(1 + \alpha_R \Delta T_W), \quad k_{e*} = k_e(1 + \alpha_k \Delta T_W). \tag{7.41}$$

The efficiency of the ball screw depends on the mechanical load of the linear drive. Its qualitative characteristics are shown in Fig. 7.20b and can be included in the model as characteristics in a lookup table. The resulting model can be computed for example in Matlab/Simulink and used for simulation and design of a controller. In this example, a cascade controller is chosen (Fig. 7.21). It consists of an inner loop for current control, a middle loop for velocity control, and an outer loop for position control. As controller for the different control loops, P- or PI-controllers are used.

7.4 Control of Teleoperation Systems

In the previous sections, an overview of system description and control aspects in general, which can be used for the design of local and global control laws, was given. The focus of this section lies on special methods used for modeling haptic systems stability analysis of bilateral telemanipulators. In contrast to Sect. 7.3, special tools for the development of control laws are presented here based on the two-port hybrid representation of bilateral telemanipulators (Sect. 7.4.1). Subsequently, in Sect. 7.4.2, a definition of transparency is introduced, which can be used to analyze the performance of a haptic system dependent on the system characteristics and the chosen control law. In Sect. 7.4.3, the general control model for telemanipulators is introduced to close the gap between the closed-loop representation, known from general control theory, and used in Sects. 7.1–7.3, and the two-port hybrid representation. In Sect. 7.4.4, it is shown how a stable and safe operation of the haptic system can be achieved. Furthermore, the design of stable control laws in the presence of time delays are presented in Sect. 7.4.5.

7.4.1 Two-Port Representation

In general, a haptic system is a bilateral telemanipulator, where a user handles a master device to control a slave device which is interacting with an environment. A common representation of a bilateral telemanipulator is the general two-port model as shown in Fig. 7.22.

User and environment are represented by one ports, characterized by their mechanical impedances $\underline{Z}_{\mathrm{H}}$ and $\underline{Z}_{\mathrm{E}}$ as they can be seen as passive elements [28], see Chap. 3. The mechanical impedance $\underline{Z}$ is defined as Eq. (7.42)

$$\underline{Z} = \frac{\underline{F}}{\underline{v}} \tag{7.42}$$

The user manipulates the master device, which controls the slave device. The slave interacts with the environment. The behavior of the telemanipulator is described by its hybrid matrix **H** [16, 37]. So the coupling of user action and interaction with the environment is described by the following hybrid matrix, taking forces and velocities at the master and slave sides and the properties of the haptic system into account.

$$\begin{pmatrix} \underline{F}_{\mathrm{H}} \\ -\underline{v}_{\mathrm{E}} \end{pmatrix} = \begin{pmatrix} \underline{h}_{11} & \underline{h}_{12} \\ \underline{h}_{21} & \underline{h}_{22} \end{pmatrix} \cdot \begin{pmatrix} \underline{v}_{\mathrm{H}} \\ \underline{F}_{\mathrm{E}} \end{pmatrix}. \tag{7.43}$$

In this case, the four h-parameters represent

$$\begin{pmatrix} \underline{F}_{\mathrm{H}} \\ -\underline{v}_{\mathrm{E}} \end{pmatrix} = \begin{pmatrix} \text{Master input impedance} & \text{Backward force gain} \\ \text{Forward velocity gain} & \text{Slave output admittance} \end{pmatrix} \cdot \begin{pmatrix} \underline{v}_{\mathrm{H}} \\ \underline{F}_{\mathrm{E}} \end{pmatrix} \tag{7.44}$$

Please note that the velocity of the slave v_E is taken into account with a negative sign. This is done to fulfill the convention for general two-ports, where the flow is always flowing into a port. The hybrid two-port representation as shown before is often used to determine stability criteria and to describe the performance properties of bilateral telemanipulators. Despite the formulation with force as flow variable (also found in [16, 30], for example), one can also find velocity as flow variable in other two-port descriptions of bilateral telemanipulators [19]. As long as the coupling is defined by the impedance formulation given in Eq. (7.42), both these variants of the two-port descriptions are interchangeable.

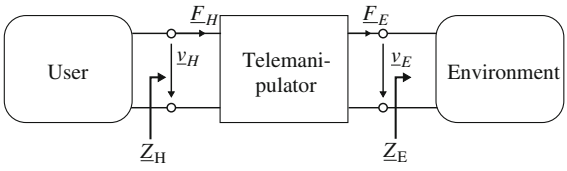

Fig. 7.22 General two-port model of a telemanipulator

7.4.2 Transparency

Besides, system stability performance is an important design criterion in the development of haptic systems. The function of a haptic system is to provide high fidelity force feedback of the contact force at the slave side to the user manipulating the master device of the telemanipulator. One parameter often used to evaluate the haptic sensation presented to the user is transparency. If the user interacts directly with the environment, he experiences a haptic sensation, which is determined by the mechanical impedance $\underline{Z}_{\mathrm{E}}$ of the environment. If the user is coupled to the environment via a telemanipulator system, he experiences a force impression, which is determined by the backward force gain and the mechanical input impedance of the master device. It is desirable that the haptic sensation for the user of the telemanipulator is the same as interacting directly with the environment. Therefore, the telemanipulator has to display the mechanical impedance of the environment $\underline{Z}_{\mathrm{E}}$ at the master device. Assume that $h_{12} = h_{21} = 1$, so there is no scaling of velocity or force. Therefore, the following conditions have to hold to reach full transparency.

$$\underline{F}_{\mathrm{H}} = \underline{F}_{\mathrm{E}} \quad \text{and} \quad \underline{v}_{\mathrm{H}} = \underline{v}_{\mathrm{E}}. \tag{7.45}$$

From this it follows that for perfect transparency [30]

$$\underline{Z}_{\mathrm{H}} = \underline{Z}_{\mathrm{E}} \tag{7.46}$$

Therefore, the force experienced by the user at the master device is

$$\underline{F}_{\mathrm{H}} = \underline{h}_{11}\underline{v}_{\mathrm{H}} + \underline{h}_{12}\underline{F}_{\mathrm{E}}$$

and for velocity at the slave side it holds that

$$-\underline{v}_{\mathrm{E}} = \underline{h}_{21}\underline{v}_{\mathrm{H}} + \underline{h}_{22}\underline{F}_{\mathrm{E}}.$$

Therefore, the mechanical impedance displayed by the master and felt by the user is described as

$$\underline{Z}_{\mathrm{T}} = \frac{\underline{F}_{\mathrm{T}}}{\underline{v}_{\mathrm{T}}} = \frac{\underline{h}_{11}\underline{v}_{\mathrm{H}} + \underline{h}_{12}\underline{F}_{\mathrm{E}}}{\frac{\underline{v}_{\mathrm{E}} - \underline{h}_{22}\underline{F}_{\mathrm{E}}}{\underline{h}_{21}}} \tag{7.47}$$

By analyzing Eq. (7.47), the conditions for perfect transparency can be derived. To achieve perfect transparency, output admittance at the slave side and input impedance at the master side have to be zero. From this it follows that for perfect transparency, in the case of no scaling, the matrix has to be of the form

$$\begin{pmatrix} \underline{F}_{\mathrm{H}} \\ -\underline{v}_{\mathrm{E}} \end{pmatrix} = \begin{pmatrix} 0 & -1 \\ 1 & 0 \end{pmatrix} \cdot \begin{pmatrix} \underline{v}_{\mathrm{H}} \\ \underline{F}_{\mathrm{E}} \end{pmatrix}.$$

It is obvious that perfect transparency is in practice not achievable without further actions taken, due to nonzero input impedance $\underline{h}_{11}$ and output admittance $\underline{h}_{22}$ of the manipulator system. If the input impedance was zero, the user would not feel the mechanical properties of the master device (mass, friction, compliance). An output admittance of zero relates to an ideal stiff slave device.

7.4.2.1 A Perception-Oriented Consideration of Transparency

Christian Hatzfeld, Sebastian Kassner, Carsten Neupert

To obtain a transparent system, the system engineer has two options: Work on the control structure, as described in the following sections or consider the perception capabilities of the human user in the definition of transparency. The latter is the focus of this section, which is based on the detailed elaborations in [22]. It has to be noted that this approach still lacks some experimental evaluation.

Up till now, transparency as defined in Eqs. (7.45) and (7.46) is a binary criterion: A system is either transparent if all conditions are fulfilled, or is not transparent if one of the equalities is not given. Despite this formulation, one can define the absolute transparency error $\underline{e}_{\mathrm{T}}$ according to HEREDIA ET AL. as shown in Eq. 7.48 [25]

$$\underline{e}_{\mathrm{T}} = \underline{Z}_{\mathrm{H}} - \underline{Z}_{\mathrm{E}} \tag{7.48}$$

and the relative transparency error $\underline{e'}_{\mathrm{T}}$ as shown in Eq. (7.49)

$$\underline{e'}_{\mathrm{T}} = \frac{\underline{Z}_{\mathrm{H}} - \underline{Z}_{\mathrm{E}}}{\underline{Z}_{\mathrm{H}}} \tag{7.49}$$

When analyzed along the whole intended dynamic range and in all relevant ↪DoF of the haptic system, Eqs. (7.48) and (7.49) allow for the quantitative comparison of different haptic systems and can give insight into the relevant ranges of frequency that have to be optimized for a more transparent system. They also provide the basis for the integration of perception properties in the assessment of transparency.

From the above-mentioned definitions of transparency [Eqs. (7.45) and (7.46)], one can conclude that $\underline{e}_{\mathrm{T}} = \underline{e'}_{\mathrm{T}} \stackrel{!}{=} 0$ to fulfill the requirement for transparency. On the other hand, it is obvious that a human user will not perceive all possible mechanical impedances, since the perception capabilities are limited as shown in Sect. 2.1. To obtain a quantified range for $\underline{e}_{\mathrm{T}}$ and $\underline{e'}_{\mathrm{T}}$, a thought experiment[1] is conducted in the following [40].

[1] Thought experiments (also *gedankenexperiment*) consider the possible outcomes of a hypothesis without actually performing the experiment, but by applying theoretical considerations. They are conducted when the actual performance of an experiment is not possible or universally valid. Famous thought experiments include Schrödinger's Cat to illustrate quantum indeterminacy.

Experiment Assumptions

The following assumptions are made for the thought experiment about the user and the teleoperation scenario:

1. Linear behavior of haptic perception as discussed in Sect. 2.1.4.2 is assumed, which holds for a wide range of tool-mediated teleoperation scenarios. Superthreshold perception properties like masking are neglected.
2. For each user, there exists a known mechanical impedance $\underline{Z}_{\text{user}}$. This impedance generally depends on external parameters like temperature, contact force as shown in Chap. 3. All of these parameters are assumed to be known and invariant over the course of the experiment. Further, a set of frequency-dependent sensory thresholds for deflection and forces exist. They are labeled as F_θ and d_θ, respectively. Both thresholds can be coupled using the mechanical impedance of the user and $\omega = 2\pi f$ as the angular frequency of the haptic signal as stated in Eq. (7.50) [23].

$$|\underline{Z}_{\text{user}}| = \left| \frac{F_\theta}{j\omega d_\theta} \right| \tag{7.50}$$

3. The user is able to impose an interaction force $\underline{F}_{\text{user,int}}$ or deflection $\underline{d}_{\text{user,int}}$ on the teleoperation system that does not necessarily trigger a sensation event at the contact point. This is, for example, possible by the movement of an arm, while only the fingertips are in contact with the teleoperation system.
4. The teleoperation system is perfectly transparent, i.e., $|\underline{e}_{\text{T}}| = 0$ for all frequencies. The system is able to read and display forces and deflections reproducible below the absolute thresholds of the user.
5. The environment is considered passive for simplification reasons.

Thought Experiment

For the experiment, an impedance type system is assumed, i.e., the user imposes a deflection on the haptic interface of the teleoperation system and interaction forces measured are displayed to the user. First, we assume an environment impedance $\underline{Z}_{\text{E}} < \underline{Z}_{\text{user}}$. Further evaluation leads to Eq. (7.51).

$$\underline{Z}_{\text{E}} = \frac{\underline{F}_{\text{E}}}{j\omega \underline{d}_{\text{E}}} < \frac{\underline{F}_{\text{user}}}{j\omega \underline{d}_{\text{user}}} = \underline{Z}_{\text{user}} \tag{7.51}$$

For an impedance type system, the user can be modeled as a source of deflection or velocity. In that case, the induced deflection of the teleoperation system equals the deflection of the environment $\underline{d}_{\text{user,int}} = \underline{d}_{\text{H}} = \underline{d}_{\text{E}}$. With Eq. (7.51), this leads to $\underline{F}_{\text{H}} = \underline{F}_{\text{E}} < \underline{F}_{\text{user}}$. Assuming that the deflection $\underline{d}_{\text{user,int}}$ imposed by the user is smaller as the user's detection threshold d_θ (assumption no. 3), the resulting amount

of force displayed to the user $|\underline{F}_{\text{user}}|$ is smaller than the individual force threshold F_θ according to Eq. (7.50).

This experiment can be extended to admittance-type systems easily. Descriptively, the result can be interpreted as the environment "evading" manipulation, as for example, a slow-moving hand in free air: The arm muscles serve as a deflection source moving the hand, but the interaction forces of the air molecules are too small to be detected.

For large environment impedances, the inequalities above are reversed. In that case, the forces or deflections resulting from the interaction are larger than the detection threshold; the user will feel an interaction with the environment.

Experiment Analysis

One can reason that the user impedance will limit the transparency error function from Eq. (7.49) from the experiment. This is done in such a way that environment impedances lower than the user impedance will be neglected as shown in Eq. (7.52).

$$\underline{e'}_{\text{T}} = \frac{\underline{Z}_{\text{H}} - \max\left(\underline{Z}_{\text{E}}, \underline{Z}_{\text{user}}\right)}{\max\left(\underline{Z}_{\text{E}}, \underline{Z}_{\text{user}}\right)} \tag{7.52}$$

If the user impedance is greater than the environment impedance, the user impedance is used, since the user will not feel any haptic stimuli generated by the lower environment impedance. If the user impedance is smaller than the environment impedance, the environment impedance is used as reference for the transparency error.

Up till now, only absolute detection thresholds were considered that describe the detection properties of haptic perception. In a second step, the discrimination properties will be considered in detail. It is assumed that a system is transparent *enough* for a satisfactory usage, if errors are smaller than the differences that can be detected by the user. This difference can be described in a conservative way by the ↪JND as defined in Sect. 2.1. With that, a limit can be imposed on Eq. (7.52) as given by Eq. (7.53)

$$\underline{e'}_{\text{T}} = \frac{\underline{Z}_{\text{t}} - \max\left(\underline{Z}_{\text{e}}, \underline{Z}_{\text{user}}\right)}{\max\left(\underline{Z}_{\text{e}}, \underline{Z}_{\text{user}}\right)} < c_{\text{JND(z)}} \tag{7.53}$$

This limit $c_{\text{JND(z)}}$ is defined as the JND of an arbitrary mechanical impedance. Although this value is not clearly measurable, it can be either bordered by the JNDs of ideal components like springs, masses, and viscous dampers (see Sect. 2.1 for values) or by the JNDs of forces and deflections (since a change in impedance can be detected if the resulting force or deformation for a fixed imposture of deflection or force, respectively, exceeds the JND). With known values, this leads to a probably sufficient limit of $\left|\underline{e'}_{\text{T}}\right| \leq 3\,\text{dB}$.

With Eq. (7.53), a perception-considering error term of the transparency of haptic teleoperation systems is given. One has to keep in mind the assumptions of the underlying thought experiment and the fact that experimental evaluation of this approach is still the focus of current research activities by the authors.

7.4.3 General Control Model for Teleoperators

In principle, a telemanipulator system can be divided into three different layers as shown in Fig. 7.23. The first layer contains the mechanical, electrical, and local control properties of the master device. The second layer represents the communication channels between the master and slave and therefore eventually occurring time delays. The third layer describes mechanical, electrical, and local control properties of the slave device. As mentioned before, the dynamic behavior of a master and accordingly a slave device (first and third layer) is determined by its mechanical and electrical characteristics. Dependent on the type of actuator used in the master device, respectively, slave device, a distinction is made between impedance and admittance devices. Impedance devices receive a force command and apply a force to their environment. By contrast, admittance devices receive a velocity command and behave as a velocity source interacting with the environment (see Chap. 6).

Customarily, dominant parameters are the mass and friction of the device. Compliance can be minimized by a well-considered mechanical design. In addition, it can be assumed that the dynamic characteristics of the electronic can be disregarded because the mechanical design is dominating the overall performance of the device. A local controller design may extend the usable frequency range of the device and can guarantee a stable operation of the device. In addition, it is possible to change the characteristics of the device from impedance behavior to admittance behavior and vice versa [19].

The second layer describes the characteristics of the communication channel. Significant physical values, which have to be transmitted between master and slave manipulator, are the values for forces and velocities at the master and slave sides.

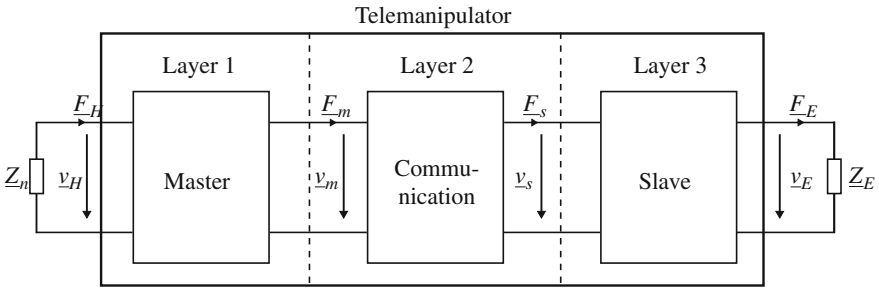

Fig. 7.23 Schematic illustration of a telemanipulator

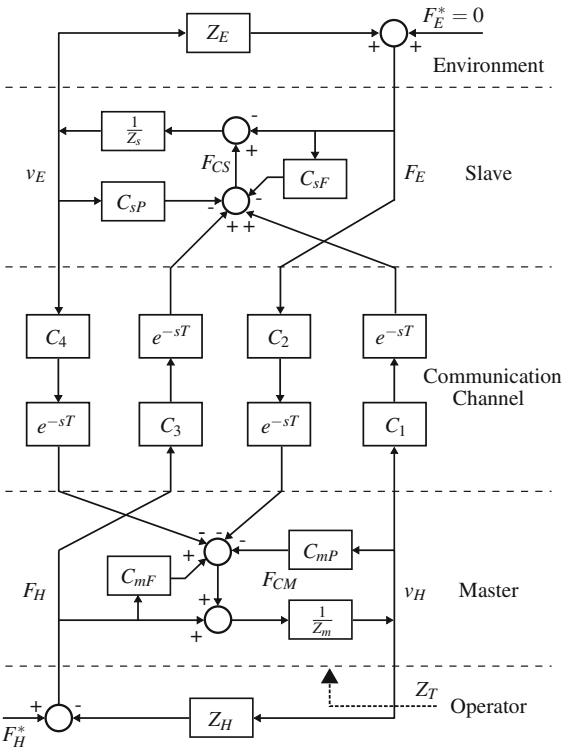

Fig. 7.24 System block diagram of a general telemanipulator in impedance–impedance architecture as shown in [21]

Therefore, telemanipulators exhibit at least two and up to four communication channels for transmitting these values. These communication paths may be afflicted with a significant time delay T, which can cause instability of the whole system.

Figure 7.24 shows the system block diagram of a general four-channel architecture bilateral telemanipulator using impedance actuators for master and slave manipulator, for instance electric motors [21, 30]. In total, there are four possible combinations of impedance and admittance devices, impedance–impedance, impedance–admittance, admittance–impedance, and admittance–admittance.

In this section, the impedance–impedance architecture is used due to its common use because of the high hardware availability. The forces of user and environment $\underline{F}_{\mathrm{H}}$ and $\underline{F}_{\mathrm{E}}$ are independent values. The mechanical impedance of user and environment is described by $\underline{Z}_{\mathrm{H}}$ and $\underline{Z}_{\mathrm{E}}$. The communication layer contains of four transmission elements C_1, C_2, C_3, and C_4 for transmitting the contact forces and velocities $\underline{v}_{\mathrm{H}}, \underline{F}_{\mathrm{E}}$, $\underline{F}_{\mathrm{H}}$, and $\underline{v}_{\mathrm{E}}$ between master and slave sides. $\underline{Z}_{\mathrm{m}}^{-1}$ and $\underline{Z}_{\mathrm{s}}^{-1}$ represent the mechanical admittance of master controller and slave manipulator. In addition, C_{mP} and C_{sP} are local master and slave position controllers and C_{mF} and C_{sF} are local force controllers.

The dynamics of the four-channel architecture are described by the following equations:

$$\underline{F}_{\mathrm{CM}} = C_{\mathrm{mF}}\underline{F}_{\mathrm{H}} - C_4 e^{-sT}\underline{v}_{\mathrm{E}} - C_2 e^{-sT}\underline{F}_{\mathrm{E}} - C_{\mathrm{mP}}\underline{v}_{\mathrm{H}}$$
$$\underline{F}_{\mathrm{CS}} = C_1 e^{-sT}\underline{v}_{\mathrm{H}} + C_3 e^{-sT}\underline{F}_{\mathrm{H}} - C_{\mathrm{sF}}\underline{F}_{\mathrm{E}} - C_{\mathrm{sP}}\underline{v}_{\mathrm{E}}$$
$$\underline{Z}_{\mathrm{s}}\underline{v}_{\mathrm{E}} = \underline{F}_{\mathrm{CS}} - \underline{F}_{\mathrm{E}}$$
$$\underline{Z}_{\mathrm{m}}\underline{v}_{\mathrm{H}} = \underline{F}_{\mathrm{CM}} + \underline{F}_{\mathrm{H}}$$

So, the closed-loop dynamics of the telemanipulator are represented by

$$\left(\underline{Z}_{\mathrm{m}} + C_{\mathrm{mP}}\right)\cdot\underline{v}_{\mathrm{H}} + C_4 e^{-sT}\underline{v}_{\mathrm{E}} = (1 + C_{\mathrm{mF}})\cdot\underline{F}_{\mathrm{H}} - C_2 e^{-sT}\underline{F}_{\mathrm{E}} \tag{7.54}$$

$$-\left(\underline{Z}_{\mathrm{s}} + C_{\mathrm{sP}}\right)\cdot\underline{v}_{\mathrm{E}} + C_1 e^{-sT}\underline{v}_{\mathrm{H}} = (1 + C_{\mathrm{sF}})\cdot\underline{F}_{\mathrm{E}} - C_3 e^{-sT}\underline{F}_{\mathrm{H}} \tag{7.55}$$

As presented in Sect. 7.4.1, it is common to describe the dynamics of a telemanipulator by two-port representation. In addition, several stability analysis methods can be applied on two-port model. From Eqs. (7.54) and (7.54) with (7.43), the following h-parameters can be obtained:

$$\underline{h}_{11} = \frac{(\underline{Z}_{\mathrm{m}} + C_{\mathrm{mP}})\cdot(\underline{Z}_{\mathrm{s}} + C_{\mathrm{sP}}) + C_1 C_4 e^{-2sT}}{(1 + C_{\mathrm{mF}})\cdot(\underline{Z}_{\mathrm{s}} + C_{\mathrm{sP}}) - C_3 C_4 e^{-2sT}} \tag{7.56}$$

$$\underline{h}_{12} = \frac{C_2(\underline{Z}_{\mathrm{s}} + C_{\mathrm{sP}})e^{-sT} - C_4(1 + C_{\mathrm{sF}})e^{-sT}}{(1 + C_{mF})\cdot(\underline{Z}_{\mathrm{s}} + C_{\mathrm{sP}}) - C_3 C_4 e^{-2sT}} \tag{7.57}$$

$$\underline{h}_{21} = -\frac{C_3(\underline{Z}_{\mathrm{m}} + C_{\mathrm{mP}})e^{-sT} + C_1(1 + C_{\mathrm{mF}})e^{-sT}}{(1 + C_{\mathrm{mF}})\cdot(\underline{Z}_{\mathrm{s}} + C_{\mathrm{sP}}) - C_3 C_4 e^{-2sT}} \tag{7.58}$$

$$\underline{h}_{22} = \frac{(1 + C_{\mathrm{sF}})\cdot(1 + C_{\mathrm{mF}}) - C_2 C_3 e^{-2sT}}{(1 + C_{\mathrm{mF}})\cdot(\underline{Z}_{\mathrm{s}} + C_{\mathrm{sP}}) - C_3 C_4 e^{-2sT}} \tag{7.59}$$

With Eqs. (7.47) and (7.56)–(7.59), the impedance transmitted to the user $\underline{Z}_{\mathrm{T}}$ is given by Eq. (7.60) [19].

$$\underline{Z}_{\mathrm{T}} = \frac{(\underline{Z}_{\mathrm{m}} + C_{\mathrm{mP}})\cdot(\underline{Z}_{\mathrm{s}} + C_{\mathrm{sP}}) + C_1 C_4 e^{-2sT} + \left[(1 + C_{sF})\cdot(\underline{Z}_{\mathrm{M}} + C_{\mathrm{mP}}) + C_1 C_2 e^{-2sT}\right]\cdot\underline{Z}_{\mathrm{E}}}{(1 + C_{\mathrm{mF}})\cdot(\underline{Z}_{\mathrm{s}} + C_{\mathrm{sP}}) - C_3 C_4 e^{-2sT} + \left[(1 + C_{\mathrm{sF}})\cdot(1 + C_{\mathrm{mF}}) + C_2 C_3 e^{-2sT}\right]\cdot\underline{Z}_{\mathrm{E}}} \tag{7.60}$$

Perfect transparency is achievable, if the time delay T is insignificant. The controllers must hold the following conditions, which are known as the transparency-optimized control law [21, 30]:

$$\begin{aligned} C_1 &= \underline{Z}_{\mathrm{s}} + C_{\mathrm{sP}} \\ C_2 &= 1 + C_{\mathrm{mF}} \\ C_3 &= 1 + C_{\mathrm{sF}} \\ C_4 &= -\left(\underline{Z}_{\mathrm{m}} + C_{\mathrm{mP}}\right) \\ C_2, C_3 &\neq 0 \end{aligned} \tag{7.61}$$

By use of local position and force controllers of master and slave C_{mp}, C_{sp}, C_{mF}, and C_{sF}, a perfect transparency can be achieved with only three communication channels. In this case, the force feedback from slave to master C_2 can be neglected [20, 21].

The most common control architecture is the forward-flow architecture [16] also known as force feedback or position-force architecture [30], which uses the two channels C_1 and C_2. C_3 and C_4 are set to zero. The position, respectively, velocity $\underline{v}_{\mathrm{h}}$ at the master manipulator is transmitted to the slave. The slave manipulator feeds back the contact forces between manipulator and environment $\underline{F}_{\mathrm{e}}$. Due to not compensated impedances of master and slave devices, perfect transparency is not achievable by telemanipulator buildup in the basic forward-flow architecture. This architecture has been described and analyzed by many authors [7, 8, 16, 17, 19, 30].

7.4.4 Stability Analysis of Teleoperators

Besides the general stability analysis for dynamic systems from Sect. 7.2, several approaches for stability analysis of haptic devices have been published. Most of them use the two-port representation introduced in Sect. 7.4.1 for stability analysis and controller design and were derived from the classical network theory and communications technology. The following section gives an introduction to the most important of them and also presents methods to guarantee stability of the system under time delay.

7.4.4.1 Passivity

The concept of passivity for dynamic systems is introduced in Sect. 7.2.2. Within this section, the focus is on the application of this concept on the stability analysis of haptic devices. Assume the two-port representation of a telemanipulator as presented in Fig. 7.23. Furthermore, it is assumed that the energy stored in the system at time $t = 0$ is $V(t = 0) = 0$. The power P_{in} at the input of the system at time t is given by the product of the force $F_{\mathrm{H}}(t)$ applied by the user to the master times the master velocity $v_{\mathrm{H}}(t)$.

$$P_{\mathrm{in}} = F_{\mathrm{H}}(t) \cdot v_{\mathrm{H}}(t)$$

Accordingly, the power P_{out} at the output of the telemanipulator is given by the contact force of the slave $F_{\text{E}}(t)$ manipulating the environment times the velocity of the slave $v_{\text{E}}(t)$

$$P_{\text{out}} = F_{\text{E}}(t) \cdot v_{\text{E}}(t)$$

Thus, the telemanipulator is passive and therefore stable as long as the following inequality is fulfilled:

$$\int_0^t (P_{\text{in}}(\tau) - P_{\text{out}}(\tau)\mathrm{d}\tau) = \int_0^t (F_{\text{H}}(\tau) \cdot v_{\text{H}}(\tau) - F_{\text{E}}(\tau) \cdot v_{\text{E}}(\tau)\mathrm{d}\tau) \geq V(t) \quad (7.62)$$

Alternatively, the criterion can be expressed in the form of the time derivative of Eq. (7.62)

$$F_{\text{H}}(t) \cdot v_{\text{H}}(t) - F_{\text{E}}(t) \cdot v_{\text{E}}(t) \geq V(t) \quad (7.63)$$

From Eq. (7.62), respectively, Eq. (7.63), it can be seen that the telemanipulator must not generate energy to be passive. Thus, an easy method to receive a stable telemanipulator system is to implement higher damping, though it decreases the performance of the system.

Considering the frequency domain passivity of the system can be analyzed using the immitance matrix of the transfer function [7, 8, 10–12, 35–37]. A system is passive and, hence inherently, stable if the immitance matrix $G(s)$ of the n-port network is positive real. The criteria for positive realness of the immitance matrix, which have to be satisfied, are [5, 24]:

1. $G(s)$ has real elements for real s;
2. The elements of $G(s)$ have no poles in $\text{Re}(s) > 0$ and poles on the $j\omega$-axis are simple, such that the associated residue matrix is nonnegative definite Hermitian;
3. For any real value of ω such that no element of $G(j\omega)$ has a pole for this value, $G(jw) + G(jw)$ is nonnegative definite Hermitian.

For real rational $G(s)$, points 1 and 3 may be replaced with

4. $G(s) + G(s)$ is nonnegative definite Hermitian in $\text{Re}(s) > 0$

User and environment can be seen as passive [28]. Therefore, if passivity of the telemanipulator system can be proved, the whole closed loop of user, telemanipulator, and environment can be guaranteed to be passive and hence stable. It has been shown that a robust (passive) control law and transparency are conflicting objectives in the design of telemanipulators [30]. In many cases, the haptic sensation presented to the user can be poor if a fixed damping value is used to guarantee passivity of the telemanipulator. Thus, a new approach using passivity-based control law and improving performance has been done by implementing a passivity observer and passivity controller. The passivity controller increases damping of the system only

when needed to guarantee stability. A further benefit of this concept is that no parameter estimation for the dynamic model of the telemanipulator has to be done and if considered, uncertainties can be compensated [18, 38].

7.4.4.2 Absolute Stability Criterion (Llewellyn)

A stability criterion for linear two-ports has been derived by LLEWELLYN [9, 24, 31]. His motivation was the investigation of generalized transmission lines and active networks. Later, several authors have used the criteria formulated by Llewellyn to analyze the stability of telemanipulators or to design control laws for bilateral teleoperation [1, 2, 4, 19]. The criterion is formulated in the frequency domain and it is assumed that the two-port is linear and time invariant, at least locally [3]. A linear two-port is absolute stable if and only if there exists no set of passive terminations for which the system is unstable.

The following criteria provide both necessary and sufficient conditions for absolute stability for linear two-ports.

1. $G(s)$ has no poles in the right half s-plane, only simple poles on the imaginary axis
2. $\mathrm{Re}(g_{11}) > 0, \mathrm{Re}(g_{22}) > 0$
3. $2 \cdot \mathrm{Re}(g_{11}) \cdot \mathrm{Re}(g_{22}) \geq |g_{12}g_{21}| + \mathrm{Re}(g_{12}g_{21}) \qquad \forall \omega \geq 0$

Conditions 1 and 2 guarantee passivity of the system when there is no coupling between master and slave. This case occurs when master or slave are free or clamped. Condition 3 guarantees stability if master and slave are coupled.

These criteria may be applied to every type of immitance matrix, thus the impedance matrix, admittance matrix, hybrid matrix, or inverse hybrid matrix. If the criteria are fulfilled for one form of immitance matrix, they are fulfilled for the other three forms as well. A network for which $h_{21} = -h_{12}$, which is the same as $z_{21} = z_{12}$ holds is said to be reciprocal. In this particular case, the tests for passivity and unconditional stability are the same. A passive network will always be absolute stable, but an absolute stable network is not necessarily passive. A two-port that is not unconditional stable is potentially unstable, but this does not mean that it is definitely unstable as shown in Fig. 7.25.

7.4.5 Effects of Time Delay

When master and slave are far apart from each other, communication data have to be transmitted over long distance with significant time delays, which can lead to instabilities unless the bandwidth of signals entering the communication block is severely limited. The reason for this is a non-passive communication block [8], so energy is generated inside the communication block.

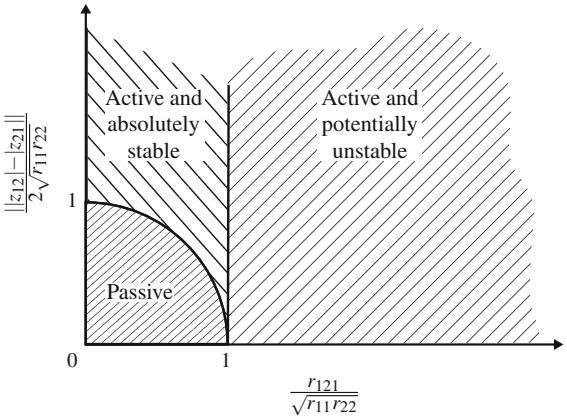

Fig. 7.25 Stability-activity diagram [24]

7.4.5.1 Scattering Theory

ANDERSON [6–8] used the scattering theory to find a stable control law for bilateral teleoperation systems with time delay. Scattering variables were well known from transmission line theory. The scattering operator S maps effort plus flow into effort minus flow and is defined in terms of an incident wave $F(t) + v(t)$ and a reflected wave $F(t) - v(t)$.

$$F(t) - v(t) = S(t)\,(F(t) + v(t))$$

For LTI systems S can be expressed in the frequency domain as follows:

$$F(s) - v(s) = S(s)\,(F(s) + v(s))$$

In the case of a two-port the scattering matrix can be related to the hybrid matrix $\mathbf{H}(s)$ by loop transformation, which leads to

$$S(s) = \begin{pmatrix} 1 & 0 \\ 0 & -1 \end{pmatrix} \cdot (\mathbf{H}(s) - 1)\,(\mathbf{H}(s) + 1)^{-1}$$

To ensure passivity of the system, the reflected wave must not carry higher energy content than the incident wave. Therefore, a system is passive if and only if the norm of its scattering operator $S(s)$ is less than or equal to one [8].

$$\|S(s)\|_\infty \leq 1$$

7.4.5.2 Wave Variables

Wave variables were used by NIEMEYER [35, 36] to design a robust control strategy for bilateral telemanipulation with time delay. It separates the total power flow into two parts, one the power flowing into the system and the other part representing the power flowing out of the system. Later, these two parts are associated with input and output waves. This approach is also valid for nonlinear systems. Assume the two-port shown in Fig. 7.26 using $\dot{x}_m$ and F_e as inputs.

Therefore, the power flow through the two-port can be written as

$$P(t) = \dot{x}_M^T F_T - \dot{x}_s^T F_S = \frac{1}{2} u_M^T u_T - \frac{1}{2} v_M^T v_T + \frac{1}{2} u_S^T u_S - \frac{1}{2} v_S^T v_S.$$

Here, the vectors $\mathbf{u}_M$ and $\mathbf{u}_S$ are input waves, which increase the power flow into the system. Analogous to this $\mathbf{v}_M$ and $\mathbf{v}_S$ are output waves decreasing the power flow into the system. Note that velocity is denoted here as $\dot{x}$. The transformation from the power variables to wave variables is described as

$$\begin{aligned} u_M &= \frac{1}{\sqrt{2b}}(F_M + b\dot{x}_M) \\ u_S &= \frac{1}{\sqrt{2b}}(F_S - b\dot{x}_S) \\ v_M &= \frac{1}{\sqrt{2b}}(F_M - b\dot{x}_M) \\ v_S &= \frac{1}{\sqrt{2b}}(F_S + b\dot{x}_S) \end{aligned}$$

The wave impedance b relates velocity to force and represents an opportunity to tune the behavior of the system. Large b values lead to an increased force feedback at the cost of high inertial forces. Small b values lower any unwanted sensations, so fast movement is possible, but also decreases the force impression of contact forces between slave and environment [34]. The wave variables can be inverted to provide the power variables as a function of the wave variables.

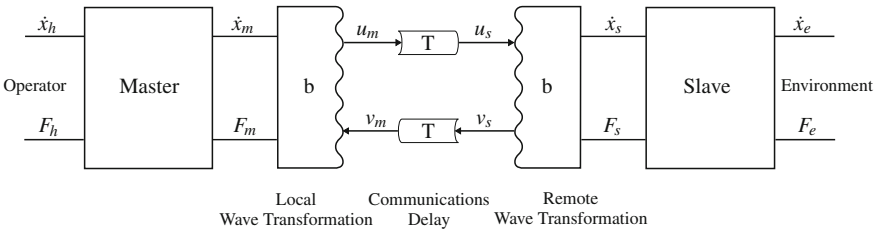

Fig. 7.26 Wave-based teleoperator model

$$F_M = \sqrt{\frac{b}{2}}(u_M + v_M)$$
$$F_S = \sqrt{\frac{b}{2}}(u_S + v_S)$$
$$\dot{x}_M = \frac{1}{\sqrt{2b}}(u_M - \dot{x}_M)$$
$$\dot{x}_S = -\frac{1}{\sqrt{2b}}(u_S + v_S)$$

By transmitting the wave variables instead of the power variables, the system remains stable even if the time delay T is not known [35]. Note that when the actual time delay T is reduced to zero, transmitting wave variables is identical to transmitting velocity and force.

7.5 Conclusion

The control design for haptic devices faces the developing engineer with a complex manifold challenge. According to the fundamental requirement, to establish a safe, reliable, and determined influence on all structures, subsystems, or processes, the haptic system composed of an analytical approach for control system design is not negligible anymore. It provides a wide variety of methods and techniques to be able to cover many issues that arise during this design process. This chapter intends to introduce the fundamental theoretical background. It shows several tasks, functions, and aspects the developer will have to focus on, as well as certain methods and techniques that are going to be useful tools for the system's analysis and the process of control design.

Starting with an abstracted view on the overall system, the control design process is based on an investigation and mathematical formulation of the system's behavior. To achieve this, a wide variety of methods exist that can be used for system description depending on the degree of complexity. Besides methods for the description of linear or linearized systems, this chapter introduced techniques for system description to represent nonlinear system behavior. Furthermore, the analysis of MIMO systems is based on the state space description, which is also presented here. All of these techniques on the one hand are aimed at the mathematical representation of the analyzed systems as exactly as possible, on the other hand they need to satisfy the requirement for a system description that further control design procedures are applicable to. These two requirements will lead to a trade-off between establishing an exact system formulation that can be used in analysis and control design procedures without extending the necessary effort unreasonably.

Within system analysis of haptic systems, the overall system stability is the most important aspect that has to be guaranteed and proven to be robust against model uncertainties. The compendium of methods for stability analysis contains techniques

applicable to linear or nonlinear system behavior, corresponding to their underlying principles that of course limit the usability. The more complex the mathematical formulation of the system becomes, the higher the effort gets for system analysis. This comes into direct conflict with the fact that a stability analysis of a system with a simplified system description can only provide a proof of stability for this simplified model of the real system. Therefore, the impact of all simplifying assumptions must be evaluated to guarantee the robustness of the system stability.

The actual objective within establishing a control scheme for haptic systems is the final design of controller and control structures that have to be implemented in the system at various levels to perform various functions. Besides the design of applicable controllers or control structures, the optimization of adjustable parameters is also part of this design process. As shown in many examples in the literature on control design, a comprehensive collection of control design techniques and optimization methods exist that enable the developer to cover the emerging challenges and satisfy various requirements within the development of haptic systems as far as automatic control is concerned.

Recommended Background Reading

[19] Hashtrudi-Zaad, K. & Salcudean, S.: **Analysis of control Architectures for Teleoperation Systems with Impedance/Admittance Master and Slave - Manipulators**. In: The International Journal of Robotics Research, SAGE Publications, 2001.
Thorough analysis of different control schemes for impedance and admittance type systems.

[26] Hirche, S. & Buss, M.: **Human perceived transparency with time delay**. In:Manuel Ferre et al. (eds.), Advances in Telerobotics, Springer, 2007.
Analysis of the effects of time delay on transparency and the perception of compliance and mass.

[41] Tavakoli, M.; Patel, R.; Moallem, M. & Aziminejad, A.: **Haptics for Teleoperated Surgical Robotic Systems**. World Scientific Publishing, Shanghai, 2008.
Description and Design of a minimal invasive surgical robot with haptic feedback including an analysis of stability issues and the effect of time delay.

References

1. Adams RJ, Hannaford B (1998) A two-port framework for the design of unconditionally stable haptic interfaces. In: Proceedings of IEEE/RSJ international conference on intelligent robots and systems, 1998, vol 2. IEEE, pp 1254–1259. doi:10.1109/IROS.1998.727471
2. Adams RJ, Hannaford B (2002) Control law design for haptic interfaces to virtual reality. IEEE Trans Control Syst Technol 10(1):3–13. doi:10.1109/87.974333

3. Adams R, Hannaford B (1999) Stable haptic interaction with virtual environments. IEEE Trans Robot Autom, 15(3):465–474. ISSN: hapt. doi:10.1109/70.768179
4. Adams R, Klowden D, Hannaford B (2000) Stable haptic interaction using the Excalibur force display. In: Proceedings of IEEE international conference on robotics and automation, ICRA 2000, vol 1. pp 770–775. doi:10.1109/ROBOT.2000.844144
5. Anderson B (1968) A simplified viewpoint of hyperstability. IEEE Trans Autom Control 13(3):292–294. doi:10.1109/TAC.1968.1098910
6. Anderson R, Spong MW (1988) Hybrid impedance control of robotic manipulators. IEEE J Robot Autom 4(5):549–556. doi:10.1109/56.20440
7. Anderson RJ, Spong MW (1992) Asymptotic stability for force reflecting teleoperators with time delay. Int J Robot Res 11(2):135–149. doi:10.1177/027836499201100204
8. Anderson R, Spong M (1989) Bilateral control of teleoperators with time delay. In: IEEE transactions on automatic control, 34(5):494–501. ISSN, pp 0018–9286, doi:10.1109/9.24201
9. Bolinder E (1975) Survey of some properties of linear networks. In: IRE Transactions on Circuit Theory, 4(3):70–78. ISSN, pp 0096–2007, doi:10.1109/TCT.1957.1086385
10. Colgate J (1993) Robust impedance shaping telemanipulation. IEEE Trans Robot Autom 9(4): 374–384. ISSN, pp 1042–296X, doi:10.1109/70.246049
11. Colgate J, Brown J (1994) Factors affecting the Z-Width of a haptic display. In: Proceedings of IEEE international conference on robotics and automation, 4:3205–3210. doi:10.1109/ROBOT.1994.351077
12. Colgate J, Stanley M, Brown J (1995) Issues in the haptic display of tool use. In: Proceedings of intelligent robots and systems international conference on human robot interaction and cooperative robots, 1995 IEEE/RSJ vol 3. pp 140–145. doi:10.1109/IROS.1995.525875
13. Föllinger O (1970) Nichtlineare regelungen 3. In: Ljapunow-Theorie and Popow-Kriterium. R. Oldenbourg Verlag GmbH
14. Föllinger O (1991) Nichtlineare regelungen 1. Grundlagen and Harmonische Balance. R, Oldenbourg Verlag GmbH. ISBN 3-486-21895-6
15. Föllinger O, (1970) Nichtlineare regelungen. 2. In: Anwendung der Zustandsebene R. Oldenbourg Verlag GmbH, 1970. ISBN: 978-3486218992
16. Hannaford B (1989) A design framework for teleoperators with kinaesthetic feedback. IEEE Trans Robot Autom 5(4):426–434. ISSN: 1042–296X. doi:10.1109/70.88057
17. Hannaford B (1989) Stability and performance tradeoffs in bi-lateral telemanipulation. In: Proceedings of IEEE international conference on robotics and automation 3:1764–1767. doi:10.1109/ROBOT.1989.100230
18. Hannaford B, Ryu J (2002) Time-domain passivity control of haptic interfaces. IEEE Trans Robot Autom 18(1):1–10. doi:10.1109/70.988969
19. Hashtrudi-Zaad K, Salcudean S (2001) Analysis of control architectures for teleoperation systems with impedance/admittance master and slave manipulators. The Int J Robot Res 20(6):419–445. doi:10.1177/02783640122067471
20. Hashtrudi-Zaad K, Salcudean SE (2002) Transparency in time-delayed systems and the effect of local force feedback for transparent teleoperation. IEEE Trans Robot Autom 18(1):108–114. doi:10.1109/70.988981
21. Hashtrudi-Zaad K, Salcudean S (1999) On the use of local force feedback for transparent teleoperation. In: IEEE international conference on robotics and automation, 3:1863–1869 doi:10.1109/ROBOT.1999.770380
22. Hatzfeld C (2013) Experimentelle analyse der menschlichen Kraftwahrnehmung als ingenieurtechnische Entwurfsgrundlage für haptische systeme. Dissertation, Technische Universität München: Dr. Hut Verlag, 2013. Darmstadt. http://tuprints.ulb.tu-darmstadt.de/3392/. ISBN: 978-3-8439-1033-0
23. Hatzfeld C, Werthschützky R (2012) Mechanical impedance as coupling parameter of force and deflection perception: experimental evaluation. In: Isokoski P, Springare J (Eds), Haptics: perception, devices, mobility, and communication. LNCS 7282. Proceedings of the Eurohaptics Conference, Tampere, FIN. Heidelberg: Springer, 2012. doi:10.1007/978-3-642-31401-8_18

24. Haykin S (1970) Active network theory, electrical engineering. Addison-Wesley, Reading ISBN:978-0201026801
25. Heredia E, Rahman T, Kumar V (1996) Adaptive teleoperation transparency based on impedance modeling. Proc SPIE 2901:2–12. doi:10.1117/12.26299
26. Hirche S, Buss M (2007) Human perceived transparency with time delay. In: Manuel Ferre et al. (eds), Advances in telerobotics, Analysis of the effects of time delay on transparency and the perception of compliance and mass, Springer, Berlin
27. Hirsch M (2013) Auswahl und entwurf eines positionsreglers unter Berücksichtigung nichtlinearer Effekte für einen parallelkinematischen Mechanismus. Diploma Thesis. Technische Universität Darmstadt, 2013
28. Hogan N (1989) Controlling impedance at the man/machine interface. In: IEEE International Conference on Robotics and Automation (ICRA). Scottsdale, AZ, USA, 1989, pp 1626–1631. doi:10.1109/ROBOT.1989.100210
29. Khalil HK (2002) Nonlinear systems. Prentice Hall, New Jersey ISBN: 0-130-67389-7
30. Lawrence D (1993) Stability and transparency in bilateral teleoperation. IEEE Trans Robot Autom 9(5):624–637. doi:10.1109/CDC.1992.371336
31. Llewellyn FB (1952) Some fundamental properties of transmission systems. In: Proceedings of the IRE 40(3):271–283. ISSN, pp 0096–8390, doi:10.1109/JRPROC.1952.273783
32. Lunze J (2005) Regelungstechnik 2. Springer, Berlin. ISBN 3-540-22177-8
33. Lunze J (2006) Regelungstechnik 1. Springer, Berlin. ISBN 3-540-28326-9
34. Niemeyer G, Preusche C, Hirzinger G (2008) Telerobotics. In: Siciliano B, Khatib O, (eds) Springer handbook of robotics. Springer, Berlin 2008, pp 741–757. doi:10.1007/978-3-540-30301-5_32
35. Niemeyer G, Slotine J-J (1991) Stable adaptive teleoperation. IEEE J Oceanic Eng 16(1):152–162. ISSN, pp 0364–9059, doi:10.1109/48.64895
36. Niemeyer G, Slotine J-J Towards force-reflecting teleoperation over the internet. In: Proceedings of IEEE international conference on robotics and automation. vol 3. IEEE. 1998, pp 1909–1915. doi:10.1109/ROBOT.1998.680592
37. Raju G, Verghese G, Sheridan T (1989) Design issues in 2-port network models of bilateral remote manipulation. In: IEEE international conference on robotics and automation (ICRA). Scottsdale, AZ, USA, 1989, pp 1316–1321. doi:10.1109/ROBOT.1989.100162
38. Ryu J-H, Kwon D-S, Hannaford B (2004) Stable teleoperation with time-domain passivity control. IEEE Trans Robot Autom 20(2):365–373. doi:10.1109/TRA.2004.824689
39. Slotine J-JE, Li W (1991) Applied nonlinear control. Prentice Hall, New Jersey. ISBN: 0-130-40890-5
40. Sorensen RA (1998) Thought experiments. Oxford University Press, Oxford, GB. ISBN 9780195129137 (Reprint)
41. Tavakoli M et al (2008) Haptics for teleoperated surgical robotic systems. World Scientific Publishing, Singapore. ISBN: 978-981-281-315-2
42. Unbehauen H (2007) Regelungstechnik II: zustandsregelungen, digitale und nichtlineare Regelsysteme Vieweg und Teubner, ISBN: 3-528-83348-3
43. Unbehauen H (2007) Regelungstechnik I. Vieweg und Teubner, ISBN: 3-834-80230-1
44. Hashtrudi-Zaad K Salcudean S (2001) Analysis of control architectures for teleoperation systems with impedance/admittance master and slave manipulators. Int J Robot Res, SAGE Publications, 2001.
45. Hirche S, Buss M (2007) Human perceived transparency with time delay. In: Advances in Telerobotics pp 191–209. doi:10.1007/978-3-540-71364-7_13
46. Tavakoli M, Patel R, Moallem M, Aziminejad A (2008) Haptics for teleoperated surgical robotic systems. Description and design of a minimal invasive surgical robot with haptic feedback including an analysis of stability issues and the effect of time delay, World Scientific Publishing, Shanghai, 2008